

CONF-760816-2

PREPRINT UCRL- 78036

Lawrence Livermore Laboratory

REVIEW OF HEAT TRANSFER PROBLEMS ASSOCIATED WITH MAGNETICALLY-CONFINED FUSION
REACTOR CONCEPTS

B. A. Hoffman, R. W. Werner, G. A. Carlson and D. N. Cornish

April 1, 1976

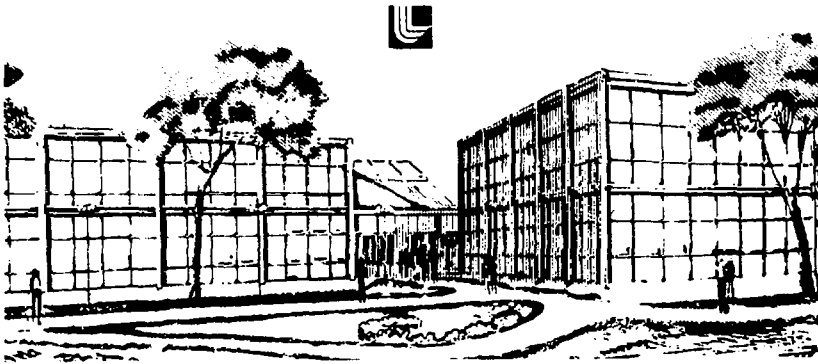
This Paper Was Prepared for Submission To:
10th National Heat Transfer Conference
St. Louis, Missouri
August 8 - 11, 1976

To be Published in:
Chemical Engineering Progress
A I Ch E Journal
International Chemical Engineering

NOTICE

PORTIONS OF THIS REPORT ARE ILLEGIBLE. It
has been reproduced from the best available
copy to permit the broadest possible avail-
ability.

This is a preprint of a paper intended for publication in a journal or proceedings. Since changes may be made before publication, this preprint is made available with the understanding that it will not be cited or reproduced without the permission of the author.



MASTER

DISTRIBUTION OF THIS DOCUMENT IS UNLIMITED

REVIEW OF HEAT TRANSFER PROBLEMS ASSOCIATED WITH MAGNETICALLY-CONFINED FUSION REACTOR CONCEPTS*

M. A. P. "Mac", W. W. Werner, G. A. Carlson, and P. W. Cornish, Lawrence Livermore Laboratory, Livermore, California U.S.A.

Acta Puer.

Conceptual design studies of possible fusion reactor configurations have revealed a host of interesting and sometimes extremely difficult heat transfer problems. The general requirements imposed on the coolant system by the several types of thermal-hydraulic power from the reactor are discussed. In particular, the requirements imposed by the fusion plasma, neutronics, structure and magnetic field environment are described. The types of heat transfer problems which are unusual or unique to fusion reactors. Then the particular requirements of the various conceivable coolants including lithium, boric, boiling Alkali metals, and helium are discussed. The extent of these general fusion reactor requirements. Some specific areas where heat transfer research in the national work is necessary are listed for each coolant along with the extent to which the research work has already been accomplished. Specialized heat transfer problems of the plasma facing components are also described. Finally, the challenging heat transfer problems associated with the reactor safety systems are reviewed, and once again some of the key unmet heat transfer needs are highlighted.

19. *Leucosia* *leucostoma* *leucostoma* *leucostoma* *leucostoma* *leucostoma* *leucostoma*

At this stage, the reactor, the first nuclear power plant in India, is to be completed and the energy generation is to begin by 1984. The reactor is to be favourably located in the northern part of the state, in the region of the northern ghats, in the state of Maharashtra. In the first phase of the programme, the first reactor will be completed in the design capacity of 200 Mw. The first thermal power plant will be followed by another two nuclear power plants, each of 200 Mw. The second and third power plants will be completed by 1987 and 1990 respectively.

Another class of nuclear reactions is the neutrino reactions. These are the reactions in which the neutrino energy present in the beta decay of the nucleus is converted into the energy of the neutrino. The neutrino energy is emitted in the form of a neutrino. The primary nuclear reactions which we consider are the beta decay reactions shown in Table I. The numbers in parentheses are the kinetic energies in Mev. of the reaction products. The neutrino reactions are shown in Table II and the neutrino-neutron reactions in Table III. The neutrino-neutron reactions are called the muon fuel cycles because they require higher reaction energies than deuterium-tritium (D-T) to achieve break-even and net power production. The potential advantage of these advanced cycles is that a large fraction of the energy of the reaction products is in the form of charged particle energy which may be directly convertible.

ionic electricity. We will consider only the less difficult D-T reaction, where 85% of the reaction energy is in the form of 14.1 MeV neutrons, and the remaining 20% is in the kinetic energy of the alpha particles (i.e., helium ions). Thus 17% of the fusion power can be directly converted.

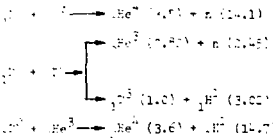


Table 1. Primary Fusion Reactions

3.1 Components of an MGR. Most of the principal components of an MGR are shown in Fig. 1.1. The thermonuclear plasma is confined by a magnetic field. Between the plasma and coil are the deuterium-deuterium blanket (labelled liquid lithium in the figure) and magnet shield. Injectors supply new deuterium and tritium fuel to the plasma. The plasma removal system is not shown. The blanket coolant is shown leaving the blanket, flowing through a heat exchanger and tritium separator, and re-entering the blanket. For the case shown, the heat exchanger transfers the heat input to a conventional steam cycle power plant. The basic physics and reactor char-

* Work performed under the auspices of the U.S. Energy Research and Development Administration under contract No. W-7405-Eng-48.

* Also, Department of Mechanical Engineering, University of California, Davis.

NOTICE
This report was prepared as an account of work
conducted by the United States Government. Neither
the United States nor the United States Energy
Research and Development Administration, nor any of
their employees, nor any of their contractors,
subcontractors, or their employees, make any
warranty, express or implied, or assume any
liability, or responsibility for the accuracy, completeness
or usefulness of any information, apparatus, product
or disclosure, or representation that the use would not
infringe privately owned rights.

acteristics for MCTR's are described in more detail in such references as Refs. 1.1 to 1.3.

1.2 Magnetic Confinement. All MCTR's confine the reacting thermonuclear plasma within a "magnetic bottle" produced by specially shaped magnet coils. At present, there are three principal magnetic field geometries being investigated for MCTR's: the Tokamak, the Mirror machine, and the toroidal Theta-Minich (see Figs. 1-1 and 1-2). Both the Tokamak and the Theta-Minich are toroidal in overall shape, with the Tokamak having a smaller ratio of major to minor radius. The Mirror machine, with its interlocking C-shaped coil coils (called Vin-Sung), is more difficult to describe, but the overall plasma geometry is roughly spherical.

1.3 The Blanket. In all of these reactors, the net neutron escape in all directions from the plasma, a neutron moderator must slow down the neutrons to convert their kinetic energy to heat for use in a thermal power cycle. To accomplish this, a blanket is normally placed between the plasma and the magnet coils (in some concepts such as the Theta-Minich, part of the magnet coils is inside the blanket). The blanket must contain "hot" neutron moderator material which is still relevant.

An equally important blanket function, unique to the MCTR cycle, is the generation of tritium at a rate that equals or preferably exceeds its consumption rate in the fusion reaction. Tritium breeding is necessary because the radioactive isotopes does not appear in any significant quantity in nature. It is proposed that tritium be bred by neutron-lithium reactions. Thus, the blanket must contain a lithium-bearing material (called the fertile material). Both naturally occurring isotopes of lithium, lithium-6 (7.3%) and lithium-7 (92.6%), react with energetic neutrons to produce tritium. The reactions are shown in Table 1...

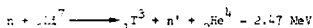
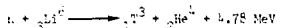


Table 1.2 - Tritium Breeding Reactions

Perhaps the most elegant concept for a blanket design is one employing molten lithium or a lithium-bearing fluid to perform all three blanket functions - neutron moderation, cooling, and tritium breeding (as implied in Fig. 1.1). However, these electrically conducting fluids are subject to magnetohydrodynamic (MHD) effects which complicate the design problem. These complications have led to proposals for use of other coolants in MCTR's. In Section 2, we discuss the various proposed blanket coolants and some of their heat transfer problems which are unique to the MCTR application.

Due to its proximity to the plasma, and because of the relatively high fraction of fusion energy which can be deposited in the first wall region, particularly during an abnormal operating conditions, there are some especially difficult

heat transfer and thermal-hydraulic design problems connected with the first wall. In some reactor designs, it is proposed to interpose a first wall shield between the plasma and the blanket first wall in order to relieve some of these problems. The heat transfer aspects of several proposed first wall shields are discussed in Section 3.

Several definitions will aid in understanding Sections 3 and 4. The blanket first wall is that surface of the blanket which is nearest the plasma. Radiant energy from the plasma and the energy of any impinging atoms or ions are deposited on the first wall. In addition, some moderation of the fusion neutrons takes place in the first wall material resulting in internal heat generation. Depending on blanket composition, the neutron energy deposition in the blanket falls off more or less exponentially from the first wall outward. The total internal heat generation in the blanket is usually more than the total neutron kinetic energy because of exothermic neutron capture reactions. The average blanket energy multiplication, M_b is defined as the ratio of the average energy generated and deposited in the blanket per neutron to 14.1 MeV, (the neutron energy at birth).

The first wall neutron loading, A_n , is defined as the current of fusion neutrons times 14.1 MeV divided by the area of the first wall, and is usually expressed in units of MW/m². Although this quantity is useful for comparisons of different reactors, the heat transfer designer must realize that it does not refer to the thermal load on the first wall since most of the neutrons penetrate to the blanket interior. (The quantity has a more direct relevance to the neutron damage problem and to the reactor economics.) Another quantity which is in common use is the total first wall loading, A_{tot} , defined as the total thermal power of the blanket divided by the first wall area. This quantity can be different for two blankets having the same A_n because of different first wall radiation flux, atom and ion impingement flux, and/or blanket.

1.4 Plasma Production, Maintenance, and Removal. Virtually all proposed processes related to the production, maintenance, and removal of the fusion plasma involve heat transfer. A primary example of a method of producing and maintaining a plasma is neutral beam injection. Neutral beam injectors are proposed for use on all Mirror reactors and most Tokamaks. They will be operated continuously on Mirror reactors and on some "driven" Tokamaks, and intermittently on self-sustaining or "ignited" Tokamaks. In general, a neutral beam injector consists of an ion source, accelerator, neutralizer, a beam direct converter for the partial recovery of the energy of accelerated ions which are not neutralized, and a vacuum system to pump excess gas from the ion source. Some of the heat transfer problems of neutral beam injectors are discussed in Section 4.

Typical plasma removal concepts for MCTR's include magnetic divertors for Tokamaks, direct converters for Mirror machines, and gas blankets

for Theta-Pinch reactors. (The gas blanket region is a gas layer surrounding the Theta-Pinch plasma for the purpose of absorbing the plasma energy and transporting it out of the plasma chamber, and is in addition to the neutron moderating blanket.) Some of the heat transfer problems of these concepts are also discussed in Section 4.

1.7 Cryogenic Heat Transfer. Most containment magnet designs for MCTR's involve the use of superconducting magnets operated at cryogenic temperatures. These magnets are subject to heating by conduction and radiation, and by nuclear penetration, and by electrical dissipation. The most common problem is to cool the magnets by the boil-off of liquid helium at atmospheric pressure and 4.2 K. Some of the heat transfer problems of liquid helium in MCTR applications are discussed in Section 6.

SECTION 1. BLANKET COOLANT THERMAL-HYDRAULIC PROBLEMS

1.1 Principal Coolant Possibilities and Limitations. In the fusion reactor concepts developed to date, the blanket coolant materials often suggested include lithium, lithium boride (Li₂BeF₄ = Ref. molten salt), liquid nitrogen and helium. Water, either boiling or pressurized, the majority of the fusion reactor concepts have not been considered a real possibility by a first generation fusion reactor, primarily because of the high pressures required. In fact, the uncertainties regarding the long-term behavior of structural materials under the intense heat and neutron bombardment of fusion reactors coupled with the desire to keep the tritium structural fraction as small as practicable for good neutron economy and tritium breeding前途 led to the search for coolant systems which result in as low pressures as possible while still yielding acceptably high heat transfer coefficients.

It is worthwhile to list some of the principal constraints including low pressures which the fusion blanket designer must consider in making his choice of heat transfer scheme and coolant:

- a) low system pressures
- b) low pumping power to thermal power ratio
- c) conservative limits on structural material stresses, corrosion and temperature
- d) convenient and efficient blanket module shape and coolant flow path geometry, and simple connectors for remote assembly and disassembly
- e) small ducting volume, number of joints and welds, etc.
- f) ease of tritium removal from the coolant and ducting
- g) efficient, high temperature energy conversion system.

All of these constraints and many more not listed make the overall conceptual design problem very complex. This complexity is well illustrated by two recent comparative studies of several fusion blanket design concepts [2.1-2.3] as well as by the many specific conceptual design studies already performed, several of which will be referenced in later sections of this review paper.

A few of the possible choices for the energy conversion system are illustrated in Fig. 2.1 (based on a figure from Ref. 2.3). As explained in Section 1, lithium or a lithium compound is required in all cases as the fertile material for breeding tritium; this lithium will also act as one of the principal neutron moderators and hence there will be substantial internal heat generation. However, in only a few cases is the fertile material proposed to be used as the blanket coolant. In the next section, we will discuss the unique magnetic effects which make it difficult to design heat transfer systems using these fertile materials as primary coolants.

As alternatives to using the fertile material as the coolant, systems using either helium or boiling potassium are suggested in the diagram. Either a conventional steam powerplant or a binary boiling potassium-steam powerplant or a direct helium gas turbine powerplant is usually proposed for generating the electricity. It seems, at first, surprising and disappointing that so exotic an energy source as nuclear fusion must probably use more or less conventional thermal powerplants. However, some direct conversion schemes for converting part of the plasma energy are being considered [2.4-2.6], and some of the heat transfer problems of these direct converters will be discussed in Section 4. The possibilities of direct energy conversion schemes are even more attractive for certain more advanced fusion reactions [2.5, 2.7].

In the following sections, we will treat first the heat transfer problems unique to the electrically conducting liquids such as lithium and zinc, and then boiling potassium and sodium, all of which experience some magnetically induced pressure drops. Then we will consider the heat transfer problems of cooling a fusion reactor with helium. Finally a comparison of the various blanket coolants will be given.

1.2 Possible Magnetic Effects on Liquid Alkali Metals and Molten Salts. Some representative property data for lithium, sodium, and potassium, and the molten salt, LiF, are listed in Table 2.1. For LiF, we have listed the properties for the 70% melting point para-eutectic [2.3, 2.8], 67% LiF and 33% BaF₂.

One of the unique problems encountered in the attempt to use these electrically conducting liquids in MCTR blankets is the effect of the strong magnetic field on the heat transfer coefficient and the pressure drop. These problems have been reviewed in some detail in references such as 2.9 to 2.14; these references also contain very useful bibliographies. In this paper, we will only review some of the principal problems created by the magnetic effects and then point out where further research is required.

When an electrically conducting fluid flows into the blanket region of a magnetically-confined fusion reactor, it will enter a region of intense magnetic field. We will consider steady-state or slowly varying magnetic fields in this discussion. (For information on some of the specialized problems of rapidly changing magnetic fields encountered in the Theta-Pinch reactor, the reader is referred to Ref. 2.15.)

Steady-state magnetic fields can produce the following MHD (magnetohydrodynamic) effects in a flowing conducting fluid:

- 1) A magnetic field component transverse to the flow direction, B_{\perp} , creates eddy currents in the moving fluid in the plane perpendicular to the fluid velocity [Fig. 2.1a] which produce a flattening of the velocity profile in the core of the flow [Fig. 2.1b] and can even produce velocity "overheads" near the walls in some cases as discussed in Refs. 2.1a and 2.1c. If the flow channel walls are electrically conducting and in good contact with the fluid, the B_{\perp} field component will also cause eddy currents to flow from the fluid through the walls as illustrated in Fig. 2.1b. These eddy currents interact with the magnetic field to create a retarding $\vec{J} \times \vec{B}$ body force on the fluid (where \vec{J} is the local current density in the fluid measured in amperes/m²). Items (a) and (b) are often referred to as "Hartmann" eddy currents. A retarding $\vec{J} \times \vec{B}$ body force can also be created by the magnetic field component parallel to the fluid motion, B_{\parallel} , if the field strength varies in the flow direction to create a radial component of the magnetic field, B_r .
- 2) If the transverse field component, B_{\perp} , varies in the flow direction (such as can occur when the flow enters or exits the magnetic field region), eddy currents in the plane perpendicular to the B_{\perp} component will be generated as illustrated in Fig. 2.1. These eddy currents are often referred to as "end-loop" eddy currents and are analogous to those generated in eddy current brakes or dampers. They cause an additional net retarding $\vec{J} \times \vec{B}$ body force on the fluid.
- 3) When a coolant duct makes a sharp bend inside the magnetic field region, magnetically induced flow separation can occur. Both the transverse and parallel components of the magnetic field induce eddy currents in turbulent flow which tend to suppress the fluid turbulence.
- 4) In a similar manner, magnetic fields tend to suppress natural convection across the magnetic field lines.
- 5) Variations of B_{\perp} or B_{\parallel} along the flow direction can cause complex variations of the temperature, air velocity profiles and turbulence distributions and hence, have a profound effect on the various flow development lengths.
- 6) Magnetic fields may have an important effect on nucleate and bulk boiling of conducting liquids in some cases.
- 7) Finally, the actual flow path may encounter combined B_{\perp} and B_{\parallel} field components which vary spatially along the flow direction in such a way as to cause complex combinations of the above effects.

This list serves to illustrate the variety and complexity of the magnetic field effects which

may be important in a particular design. To date, experiments have verified the existence of essentially all of these effects, but quantitative design information is very incomplete.

Before listing some of the specific areas where further research is required, examples of two of the important magnetic effects where reasonable experimental verification exists will be reviewed. We will consider the simplified situation of steady flow in constant area ducts in uniform, steady magnetic fields. These are:

Example 1) Effect of turbulence suppression by a pure B_{\perp} or B_{\parallel} field component (Item (a) above) or the heat transfer coefficient.

Example 2) Effect of a uniform B_{\perp} or B_{\parallel} field component on the pressure drop (Items (a) and (b) above).

Example (1): Magnetic Turbulence Suppression. Experimental evidence [2.16-2.18] indicates that a strong B_{\perp} field can completely suppress the fluid turbulence provided the field strength is above a critical value given by:

$$H_{\perp} (a) \geq \frac{Re(D_h)}{K_1}$$

where $H_{\perp} (a) = B_{\perp} \sqrt{\frac{a}{\mu}}$ = transverse Hartmann number, a is the pipe radius (or the half-height of a rectangular duct in the B_{\perp} direction), μ the fluid electrical conductivity and ν the fluid viscosity. Values of K_1 ranging from about .367 to 500 have been proposed depending on the aspect ratio of the wet cross-section and to some extent, the experimental conditions. For nearly square ducts and for round pipes, the most widely quoted values of K_1 seem to lie between 300 [2.16] and 500 [2.16].

For a highly electrically conducting fluid such as liquid lithium flowing in a 2-cm diameter duct across a 10-tesla field, H_{\perp} is almost 10,000. This implies full turbulence suppression (i.e. full magnetic laminarization) in MTR applications.

Even for a slightly electrically conducting fluid such as fibre, the transverse Hartmann number, H_{\perp} , is on the order of 40 to 50 for typical flow conditions in a 10-tesla field. Consequently, the flow would be magnetically laminarized up to Reynolds numbers of at least $300 \times 40 = 1.2 \times 10^4$ for these conditions, and we see that even fibre can experience full turbulence suppression in strong enough transverse magnetic fields.

For the case of a B_{\parallel} field, the experimental results [2.19, 2.20] are less complete as illustrated by Fig. 2.5. (Additional experimental results are presented in Refs. 2.1a and 2.14.) Since parallel Hartmann numbers, H_{\parallel} (defined in an analogous manner to H_{\perp}) over 10,000 can be encountered in fusion reactors using the liquid alkali metal coolants, a substantial extrapolation

tion of the available data is required, as illustrated in Fig. 2.5. For high H_1 , the estimates of Figs. 2.9 and 2.14 are that the maximum turbulence suppression possible in a parallel field occurs for

$$B_{||} (a) \geq \frac{Re(B_{||})}{H_1}$$

where $Re(B_{||})$ is about 40 when $H_1 > 100$. However, even at these high values of H_1 , the turbulence is never fully suppressed in the core of the flow. (See Figs. 2.10 and 2.14 for a more detailed discussion.)

Any significant degree of turbulence suppression can typically have a profound effect on the heat transfer capability of coolants. In the limiting case of an incompressible fluid, turbulence suppression by either $B_{||}$ or B_{\perp} is small, which is highly problematic for liquid metal coolants in the MTR environment. The Nusselt number can be reduced to values as low as 0.3 (for a parabolic velocity profile) in a duct in the limiting case of $Re(B_{||}) = 1$ [2.11]. In addition, the Nusselt number can vary significantly around the circumference of a round tube in a $B_{||}$ field [2.11].

An estimate of the effect of partial turbulence suppression due to a $B_{||}$ field on the Nusselt number is given in Ref. 2.11:

$$Nu_p = Nu_0 - 0.035 Re^{-1} \left[\frac{1}{1 + 1600 \left(\frac{B_{||}}{B_{||0}} \right)} \right]^{1.7}$$

where the ordinary turbulent Nusselt number data was represented by the empirical equation: $Nu_0 = 0.035 Re^{0.75} (For B_{||} = 0)$ and where

$B_{||0} = 4 B_{||}$. This semi-empirical relation is based on limited experimental data with liquid gallium ($Fr = 0.033$) in round tubes over a range of Reynolds numbers from 3×10^3 to about 10^5 and Hartmann numbers H_1 (a) of 190 and 270. While the equations for Nu_0 and Nu_p fit the limited experimental data well, additional experimental data are required to extend it outside this range.

The turbulence suppression can also have an effect on the friction coefficient and hence on the pressure drop. However, this is usually of secondary importance in fusion reactor situations, where one or more of the effects in Items (a) through (c) usually dominates. This will be discussed in the next section.

Example (2): Magnetic Pressure Drops. A transverse magnetic field, B_{\perp} , results in a pressure gradient given by the following approximate equation [2.9]:

$$-\frac{a^2}{uu} \frac{dp}{dx} = K_0 \left[-\frac{a^2}{uu} \frac{dp}{dx} \Big|_{B=0} + \frac{H_1 \tanh H_1}{H_1 - \tanh H_1} - 3 + \frac{H_1^2 C}{14C} \right]$$

where K_0 is a coefficient (on the order of unity) which depends on the duct cross-section geometry as well as on C and H_1 [2.23]. The first term on the right-hand side represents the ordinary frictional pressure gradient for the particular duct cross-section. The second and third terms account in an approximate way for the steepening of the velocity profile at the wall due to Effect (a) listed at the beginning of this section. The last term accounts for the additional pressure gradient caused by the magnetic body forces due to electrically conducting duct walls, Effect (b).

The wall conductance ratio $C = \frac{\sigma_w}{\sigma_a}$, where σ_w is the wall electrical conductivity and σ_a is the effective wall thickness.

For the usual high transverse Hartmann numbers of highly electrically conducting fluids such as liquid alkali metals in MTR conceptual designs, the last term dominates even for the minimum conceivable values of C of about 0.01 for very thin-conducting walls. Only if some way is found to produce electrically insulating walls or coatings which are compatible with the coolant and can survive the intense neutron bombardment for a sufficient length of time, will the other terms become dominant. For typical liquid alkali metal flows, the pressure drops caused by the magnetic body forces can be three to six orders of magnitude higher than the ordinary frictional pressure drops [2.9].

These dramatically large magnetic pressure drops can either result in excessive pumping power requirements or in excessive duct wall stresses near the flow inlets or both [2.9, 2.11, 2.13], depending on the detailed flow paths and magnetic field variations of a specific design.

The magnetic pressure drop in round tubes with electrically insulating walls has been well verified for the uniform $B_{||}$ field case [2.9, 2.11, 2.16-2.18]. The effect of electrically conducting tube walls has also been confirmed recently as shown in Fig. 3.6 from Ref. 2.23, and inconsistencies in earlier experiments have been clarified in that reference.

For the case of a slightly electrically conducting fluid such as flibe, the maximum H_1 (a) would probably not exceed 50 for $B_{||}$ as high as 10 tesla and the duct half-height, a , on the order of a few centimeters. However, the wall conductance ratios, C , are very much larger than unity for flibe due to its low electrical conductivity compared to most metallic wall materials proposed. In spite of this high value of C , the low value of H_1 for flibe normally results in quite small magnetic effects on the pressure drop in current MTR conceptual designs [2.13].

In sharp contrast to the case of a uniform $B_{||}$

field, a purely longitudinal magnetic field aligned parallel to the flow direction, $B_{||}$, will induce no eddy currents as long as $B_{||}$, the flow channel area, and the velocity profile do not change in the flow direction. Consequently, there will be no magnetic body forces to cause additional large pressure drops even for liquid metals. In fact, as discussed in the preceding section, the turbulence suppression due to $B_{||}$ will tend to laminarize a turbulent flow, and hence reduce the frictional pressure drop somewhat. The exact value of the friction factor in this case would depend on the velocity profile as well as the degree of turbulence suppression. For example, for strong turbulence suppression, the velocity profile would undergo a gradual transition from the ordinary turbulent velocity profile to the laminar velocity profile if sufficiently long flow lengths were available.

We may summarize the preceding discussion regarding the two coolants, lithium and flibe:

- a) Liquid lithium (and other liquid alkali metals as well) will probably experience full magnetic turbulence suppression along a good portion of the flow path in the MCTR applications. This will lower the heat transfer coefficients to the laminar values.
- b) Flibe, due to its low electrical conductivity, will probably only experience full magnetic turbulence suppression in regions of very strong transverse magnetic fields. In these circumstances, flibe has an exceedingly poor (laminar) heat transfer coefficient due to its low thermal conductivity.
- c) However, by virtue of its low electrical conductivity, flibe should not experience significant magnetic pressure drop.
- d) Lithium (and other liquid metals) may experience magnetic pressure gradients three to six orders of magnitude higher than the ordinary frictional pressure gradients. This creates a difficult thermal-hydraulic design problem with regard to duct wall stresses or pumping power required or both.

2.1 Discussion of Research Problem Areas for Electrically Conducting Coolants. These two examples serve to illustrate some of the important thermal-hydraulic effects of magnetic fields on electrically conducting fluids in rather idealized situations. In actual conceptual design studies performed to date using lithium as a primary coolant, the flow paths tend to encounter spatially varying B_{\perp} and $B_{||}$ field components as well as varying duct cross-sectional areas. Figure 2.7 illustrates a portion of the University of Wisconsin conceptual design for their UWAK-I toroidal fusion reactor [2,24], while Fig. 2.8a and b illustrate the flow turnaround region in a Lawrence Livermore Laboratory mirror fusion reactor design study [2,25]. Fig. 2.9 shows a cross-section of the module in the Culham toroidal reactor design [2,26]. Each of these particular conceptual designs exhibits some unique problems related to the magnetic effects on the liquid lithium coolant.

In the case of the Princeton reference tokamak design [2,27], flibe is used as an "auxiliary" internal heat transfer fluid inside the blanket region, as well as the fertile material for trit-

ium breeding. (Helium is used as the primary heat removal fluid.) A cross-section of the flow paths in this design is shown in Fig. 2.10. The interested reader is referred to the full reports for more details.

Detailed conceptual design studies such as these have served to identify important problems with the use of "heat coolants" and to point out areas where design information is lacking. Following is a list of some of the key areas where additional research on magnetic effects due to both uniform and nonuniform B_{\perp} and $B_{||}$ magnetic field components is required:

- a) Study of the effect on the hydraulic and thermal development lengths of representative magnetic field variations along the flow path, and the resulting effects on the local and average heat transfer coefficients and pressure gradients.
- b) Additional experiments on the effects of very high magnetic interactions on both end loop and Hartmann type eddy currents and the resulting effects on the local heat transfer coefficients and pressure gradients.
- c) The effect on local heat transfer coefficients and pressure drops under conditions where magnetically induced separation in straight ducts, bends and turnarounds is likely to occur.
- d) Effect of combined end-loop type eddy currents and hartmann type eddy currents on heat transfer coefficients and pressure gradients.
- e) More exact determination of the values of the K_{\perp} and $K_{||}$ in the ranges of Re , Pr , $H_{||}$, H_{\perp} , C and duct cross-section shapes of interest to MCTR applications.
- f) Transient thermal-hydraulic behavior (e.g., during start-up, shutdown, or emergency cooling conditions) of electrically conducting fluids in MCTR fusion reactor geometries and operating conditions.
- g) Effects of magnetic pressure drops on the performance of high temperature heat pipes. In Ref. 2,28, Werner proposed an advanced modular blanket concept utilizing heat pipes. Since the working fluid in the heat pipes will be a liquid metal such as potassium or sodium, there will be magnetic pressure drops in the liquid flow in the wick structure. Predictions of these magnetic pressure drops in Ref. 2,29 need to be verified experimentally (one such research program is not under way at the Lawrence Livermore Laboratory).

The above list should serve to point out that many of the above problem areas are unfortunately quite design dependent. It will require great ingenuity to devise experiments of broad applicability, and to develop simple enough semi-empirical equations and/or graphical presentations of the results to be useful in design work.

The detailed MCTR conceptual design studies performed to date indicate that it is very difficult to use lithium or flibe as primary coolants. Because of the difficulties, many workers in this field have looked into alternative coolant possibilities. Some of these alternative coolants will be discussed in the next two sections.

2.4 Boiling Liquid Metal Coolants. It has been proposed to use boiling liquid metals as the primary heat removal fluid in MCTR designs to achieve both improved heat transfer and substantial reductions in the magnetic pressure drops. One conceptual design study of a fusion reactor blanket using boiling potassium has already been done [1,2,3,4]. A cross-section of the proposed blanket is shown in Fig. 2.1. In this design, lithium is used as the internal heat transfer fluid (as well as the fertile material); it is circulated by internal MTR pumps [2,30,31]. Boiling potassium serves to remove the thermal energy from the blanket to the energy conversion system. A sub-scale experiment to demonstrate the lithium portion of the concept has been run [1,31].

For the portion of the potassium flow path where the fluid temperature is below the onset of sub-cooled nucleate boiling, it is affected by the magnetic field in the same way as any electrically conducting fluid. In addition, the magnetic field may have some effect on:

- (1) the onset of nucleate boiling
- (2) the effective heat transfer in the nucleate boiling regime
- (3) the transition to bulk boiling
- (4) the nature of the flow in the bulk boiling regime
- (5) the critical heat flux.

Once the void fraction reaches about 50%, the average heat-removal conductivity of the two-phase fluid becomes so low that negligible eddy currents can be induced. Consequently, the major portion of the bulk boiling regime may be unaffected by the magnetic fields. However, in the initial phases of bulk boiling, an annular film of liquid moving across magnetic field lines would induce some eddy currents in the liquid which might, in certain circumstances, affect the flow.

To the authors' knowledge, only one experiment has been performed to investigate the effect of magnetic fields on boiling liquid metals [1,34]. The experiment involved a vertical tube of potassium in a solenoidal magnet such that the B field was also vertical. Nucleate boiling was produced near the bottom of the tube, such that the bubbles had to push liquid across the field lines as they grew at the nucleation sites. Once the bubbles broke away, they travelled upward parallel to the B field. Magnetic fields as high as 1 T were used in these experiments. The results indicated little or no effect of these strong magnetic fields on the nucleate boiling process.

Additional experiments should be run under forced convection, nucleate boiling conditions at various orientations to the gravity field to check these pool boiling results. In addition, experiments in the bulk boiling regime are probably warranted, particularly to see if there are any magnetic effects on the "critical heat flux."

2.5 Gaseous Helium Coolant. Of all the possible gaseous coolants, helium is the only one which has been considered in detailed MCTR conceptual design studies to date. This initial choice has undoubtedly been strongly influenced by the HTGR (high temperature gas-cooled fission reactor) experience. Helium has some well known advan-

tages, including high heat transfer coefficients, negligible nuclear activation, chemical inertness, and it is completely unaffected by magnetic fields at the temperatures of current interest (on the order of 900-1200 K).

From a general point of view, helium has few, if any, heat transfer problems which are unique to the fusion reactor application. However, the proposed flow path geometries in specific fusion reactor conceptual designs are generally more complicated than in HTGRs, and the internal heat generation in the blanket is much more nonuniform.

Even ignoring the complications of specific designs, parametric studies such as those of Refs. 2.35 to 2.37 indicate that there are quite severe limitations on the tube lengths and diameters which can be used if good heat transfer with reasonable tube wall temperatures and stresses, as well as reasonable helium pressures, pressure drops and pumping power are to be achieved, particularly in the first wall region facing the plasma. Fig. 2.12 illustrates some of these constraints for a reactor first wall made up of a simple array of parallel tubes [2,36]. The limit on the maximum allowable stress fixes an upper limit of about 2.5 cm on the tube diameter for this example. A maximum allowable tube wall temperature determines the minimum permissible tube lengths for each tube diameter for a specific bulk temperature rise. Finally, a maximum allowable ratio of pumping power to thermal power determines the maximum permissible tube lengths for each tube diameter. These three constraints define the "permissible region" of Fig. 2.12.

Specific MCTR conceptual design studies have revealed additional heat-transfer-related problems with helium which are primarily related to the size of the inlet and outlet ducting required and the number of tube joints and welds required. These problems are illustrated in Table 2.2 based on data taken from Ref. 2.1. Shown are some estimates of the number of joints, length of welded seam and mean time between leaks for two ORNL (Oak Ridge National Laboratory) designs, the first of Ref. 2.31 cooled by boiling potassium, and the second an earlier design cooled by helium [2,37]. The estimates indicate that the helium-cooled design has less than one fifth the mean time between leaks of the boiling potassium cooled design. In addition, in these designs, the helium requires about ten times the flow passage area and about seven times the pumping power. However, these values are highly design-dependent, and improved helium designs are undoubtedly possible.

Another type of heat-transfer problem with helium is related to the specific geometry of the blanket modules or segments selected. Figure 2.13 shows the complex tubing geometry used in a version of the Culham design of Fig. 2.3 which employs helium as the primary coolant in place of lithium [2,38].

If simpler helium flow paths are desired in relatively small modules, the lithium and other blanket materials may have to be canned. Figure 2.11 from the Lawrence Livermore Laboratory mirror-fission hybrid design study [2,39] had a down flow of helium around the outer annular region, a turn-around region containing clad

lithium compounds and other fertile and fissile materials. However, this simple flow path resulted in poor heat transfer coefficients in the critical first wall region, and some redesign of the helium flow path in this region would probably be necessary. Due to the possibility of flow separations and recirculation near the critical first wall region, experimental verification of the estimated heat transfer coefficients for the particular geometry chosen would be imperative.

Other possible helium flow paths and modularization concepts for toroidal reactors are illustrated in Figs. 2.10, 2.15, and 2.16 from the conceptual design studies in Refs. 2.27, 2.40, 2.41, respectively. Reference 2.42 discusses some of the difficult problems of module design for ease of assembly and disassembly for a magnetic mirror reactor. The reader is referred to these references for more details.

5. Other Possible Coolants. In addition to the coolants proposed in the Jetetulid MCTR conceptual design studies performed to date, a few other possibilities have been mentioned in the literature. A recent paper [2.43] proposed using helium with a high loading (as much as 30% by weight) of lithium oxide dust as the coolant plus tritium breeder (i.e. the fertile material). This concept was proposed in an attempt to simplify the tritium removal problem and to reduce the tritium inventory in the reactor. Much experimental research is clearly required in order to define the transient as well as steady thermal-hydraulic behavior of this type of two-phase flow in a duct with many turns and possibly even sharp bends. In particular, dust collection in stagnation regions, slinkier formation and the problem of hot spots would have to be investigated.

Other gaseous coolants such as argon, neon, carbon dioxide and so forth are additional possibilities, although they are not considered prime candidates today.

5.7 Comparison of Coolants. As a first step, the heat transfer coefficients of the most promising coolants can be compared. Figure 2.17 shows a comparison of the heat transfer parameter, $Hu \times \delta$, for several important initial cases as a function of Reynolds number [2.10]. This figure graphically demonstrates the very detrimental effect that full magnetic laminarization would have on tube and to a lesser extent on lithium if operation at moderate to high Reynolds numbers were required. However, the figure is somewhat misleading if one tries to use it to make a direct comparison among the various coolants, since each coolant would be used at a different Reynolds number.

One of the most interesting and revealing studies to date which compares the heat transfer and thermal-hydraulic aspects of the most promising MCTR coolants in a self-consistent manner is that of Ref. 2.13. One of the two "reference designs" used in that reference to make the comparison, the tubular or ducted design, is shown in Fig. 2.18. The authors chose the common reference conditions shown in Table 2.3 and then calculated the velocities, heat transfer coefficients, pressure drops and pumping power requirements for each coolant as a function of the total wall

loading, A_T , (defined in Section 1).

Typical Reynolds numbers and transverse Hartmann numbers for the various coolants are listed in Table 2.3 as well as the pertinent results for the reactor thermal-hydraulic performance for a total wall loading of 1 MW/m^2 . It is assumed in Ref. 2.13 that 30% of this thermal power is absorbed by the coolant flowing in the array of round tubes which makes up the first wall of this hypothetical reactor. It should be clear that this highly simplified coolant geometry is only useful for the purpose of comparing potential coolants and is not intended to represent a real "design". As pointed out in Ref. 2.13, a good designer may be able to minimize or eliminate entirely many of the problems revealed by this comparison.

The resultant pressure drops are shown in Fig. 2.19 for the entire spectrum of wall loadings studied. For $A_T = 1 \text{ MW/m}^2$, the pumping power ratios were given in Ref. 2.13 as 5.5%, 15% and 35% for liquid lithium, boiling sodium and boiling potassium, respectively. For the boiling coolants, these relatively large pumping powers are due in part to the fact that the coolants flow across the strong magnetic fields (10 T) as liquids for several meters before beginning to boil and in part to the high velocity and low density of the vapor.

It should be noted that if one is able to use preheating of the sodium or potassium before it enters the magnetic field region, it should be possible to greatly reduce the magnetic pressure drops (or even eliminate them by preheating to a void fraction of about 85% or more before entering the magnetic fields).

The corresponding heat transfer parameters are shown in Fig. 2.20 as a function of the total wall loading (from Ref. 2.14 for the specific numerical conditions of the study of Ref. 2.13). This figure reveals that even if the tube flow were in the ordinary turbulent flow regime, it apparently would have much lower heat transfer coefficients than lithium or helium for a given wall loading. The authors of Ref. 2.13 point out that the tube velocities could be increased substantially without incurring excessive pressure drops. This might improve the heat transfer coefficients if the tube is not fully laminarized by the magnetic fields. However, then electrolytic corrosion might become unacceptable when the induced voltage exceeds about 1 volt (based on the data of Ref. 2.8).

The recent comparative study [2.1] of several different MCTR conceptual designs employing several different coolants goes well beyond the limited scope of comparing thermal-hydraulic capabilities. The author has attempted the much more ambitious task of comparing how the designs meet all the various MCTR constraints. The author has made a good beginning, and his report should be required reading for anyone intending to work in this field. His study reveals the enormity of some of the problems related to tritium holdup and separation, ducting volume, joints and welds required, reliability and maintainability, all of which are strongly coupled to the choice

of coolant and the detailed design of the heat removal and energy conversion system.

Other crucial blanket heat transfer problem areas mentioned in Ref. 1.1 which have received scant attention to date include:

- (1) transfer startup and shutdown cooling
- (2) plasma dump to the first wall
- (3) afterheat and emergency blanket cooling
- (4) coolant leakage detection and partial shutdown of one or more modules.

SECTION 3. FIRST WALL SHIELDS

3.1. Introduction. In several reactor designs, it is proposed to interpose a first wall shield between the plasma and the first wall of the blanket in order to relieve some of the difficult heat transfer and thermal-hydraulic-structural design problems associated with the first wall. The functions and designs of various first wall shields is now different considerably. In this section, we will briefly discuss the heat transfer aspects of three proposed first wall shields --- the carbon curtain of the URAK-II Tokamak reactor [3.1], the carbon spectrum shifter of the URAK-III Tokamak reactor [3.2], and the water-cooled first wall shield of the mirror FERF (Fusion Engineering Research Facility) [3.3].

3.1.1. URAK-II Carbon Curtain. The carbon curtain concept was developed to reduce the radiation loss from the plasma of the URAK-II Tokamak reactor [3.1]. In tokamak plasmas, ions with high atomic number, such as neutron-sputtered first wall atoms, will diffuse inward and greatly increase the radiation loss compared to that of a pure D-T plasma. It is clear that lower Z impurities (e.g., C, O, Si, etc.) have a much less serious impact on plasma performance than the heavier metallic atoms. The URAK-II carbon curtain is a flexible, two-dimensionally woven carbon cloth placed between the plasma and the metallic first wall. It is claimed that this cloth will intercept practically all ion and neutral atoms leaking from the plasma and prevent metallic ions which emanate from the first wall from entering the plasma.

The carbon curtain is to be cooled by thermal radiation to the first wall. The maximum allowable temperature for the curtain is about 2000°C, above which the vapor pressure of carbon would exceed the maximum allowable background pressure in the plasma chamber. In the URAK-II design, the estimated 10 kW/cm^2 heat load on the curtain results in a 660°C curtain temperature for a first wall temperature of 600°C and an effective emissivity of unity (not 0.5 as stated in Ref. 3.1). For the same emissivity and first wall temperature, the maximum allowable temperature of 2000°C would be reached with a heat flux of 150 W/cm^2 .

3.1.2. URAK-III Spectrum Shifter. In the URAK-III conceptual design [3.2], the first wall is separated from the plasma by a thick carbon shield which may be made of three-dimensionally woven carbon cloth. This shield has the same advantages as the two-dimensional carbon curtain, but in addition, softens the incident neutron spectrum, resulting in reduced gas production and atom displacement rates in the first wall

and blanket. It is estimated that the spectrum shifter will extend the life of the first wall in URAK-III by a factor of 5.

The heat load on this shield is greater than that for the carbon curtain because of significant neutron heating. However, it is presently proposed to passively cool the spectrum shifter in the same manner as the carbon curtain --- by thermal radiation to the first wall. An alternative proposal to attach the spectrum shifter to the first wall with heat pipes is being investigated [3.4]. If the heat pipes use an electrically conducting fluid, they will be subject to the effects discussed in Sections 2.2 and 2.3.

3.1. FERF First Wall Shield. The mirror FERF (Fusion Engineering Research Facility) [3.3] is a small non-power-producing mirror reactor proposed for testing and evaluating the materials and components which will be used in early fusion reactors. It is designed to produce a high 14.1 MeV neutron flux ($> 10^{12} \text{ neutron/cm}^2/\text{s}$) over an area large enough to accommodate engineering-scale test specimens (several square meters). Because of the smallness of this reactor, a considerable fraction of the injected neutral beam power is lost to the first wall in the form of energetic injected neutrals which penetrate through the plasma as well as other energetic neutrals resulting from charge exchange collisions between injected neutrals and plasma ions. Analysis predicts that the peak (and average) power flux of energetic neutral atoms to the first wall of FERF will be 3.3 kW/cm^2 (and

1.3 kW/cm^2 with no plasma present at the beginning of buildup), and 790 W/cm^2 (and

210 W/cm^2 in steady state. It should be noted that larger mirror reactors will have very much lower steady state neutral atom power fluxes, although they may have transient power fluxes similar to FERF. This difference opens up additional possibilities for the solution of the heat transfer problems.

In order to handle the high power fluxes for FERF, it is proposed to use a first wall shield consisting of an array of thin-walled tubes carrying high velocity water in the non-boiling or subcooled nucleate boiling regime. Such a shield would have very little effect on the 14.1 MeV neutrons, and thus would not invalidate the testing of materials and components behind the shield.

A thermal-hydraulic analysis of such a first wall shield [3.5] has indicated that:

a) With the use of a high-temperature alloy such as Ti-10W, heat flux capabilities as

high as 3.3 kW/cm^2 seem entirely feasible in 1 meter long tubular wall sections (using tubes with an inner diameter of 10 mm and wall thicknesses of 0.5 mm with a structural safety factor of 1.0). The predicted performance of these tubes for various heat fluxes is shown in Fig. 3.1.

b) The pumping power requirements are reasonable for an early experimental fusion machine even in the non-boiling flow regime (less than 1 MW per square metre of first

wall area exposed to the high energy flux).

c) Lower flow rates and pumping powers are required in the subcooled nucleate boiling regime (pumping power as much as an order of magnitude lower). However, uncertainties in the empirical equations used to model the subcooled boiling regime at these high mass flow rates and high heat fluxes, particularly the pressure gradient equations, indicate that some experimental verification of these predictions would be necessary before using the results in design.

d) Even higher heat flux capabilities are possible with lower structural safety factors. For example, if the safety factor can be lowered from 1.0 to 0.5, the maximum allowable heat flux on the 1 m long tube is increased from 3500 to about 4000 W/cm² (see Fig. 3.1).

SECTION 4. INJECTORS, DIVERTORS AND DIRECT CYCLES

4.1. Introduction. To describe the heat transfer problems appropriate to these three regions of a fusion reactor, we may categorize magnetically confined systems into two broad extremes:

- 1) those with plasmas that are relatively "poorly confined" [4.1],
- 2) those with plasmas that are relatively "well confined" [4.1].

They may be further categorized as machines that are (a) pulsed, (b, c, d) or (e) steady-state [4.1]. Whatever the combination may be, there are certain prerequisites in handling energy injection and energy recovery (which we term as "circulating power" that must be satisfied to produce net fusion power. These prerequisites create a significant number of interesting heat transfer problems.

If we start discussing relatively "poorly confined" plasmas typified by Mirror machines, it will be seen that there is involved a large amount of circulating power; this power, in fact, may be three or more times the useful reactor power output delivered to the electrical grid (see Fig. 4.1). This is far from ideal situation arises because the Q of Mirror machines based on the current state of mirror confinement physics is approximately unity [4.6]. The definition of Q is:

$$Q = \frac{\text{Thermonuclear Power}}{\text{Injected Power}}$$

The thermonuclear power is derived from the D-T fusion reaction yielding 14.1 MeV neutrons and 3.5 MeV alpha particles as was indicated in Table 4.1. The mirror machine is a driven power amplifier where the overall power output is then $(P_{\text{inj}} + Q P_{\text{inj}})$. With a Q of 1, the amplification is low. If the efficiency of energy recovery is specified by η_R and the efficiency of injection is η_{inj} , then breakeven, the point that must be exceeded for commercial interest, is specified by:

$$(1 + Q) \eta_R \eta_{\text{inj}} = 1.$$

It can be seen from this simple equation that in Mirror machine reactors based on current low values of Q, as high a value of η_R as possible must be obtained for a favorable energy balance. The value of η_R can be substantially increased by utilizing direct conversion. By including direct conversion, the overall efficiency is improved over that of a thermal cycle as follows:

$$\eta_{\text{DC}} = \eta_{\text{DC}} + (1 - \eta_{\text{DC}}) \eta_{\text{TH}}$$

where η_{DC} is the part of η_R applicable to the charged particle power (~ 20% of the total thermonuclear power plus the unreacted plasma). This equation is, in reality, the equation for a binary topping cycle. A demonstrable overall efficiency value in a direct converter with a thermal bottoming plant would be [4.7]:

$$\eta_{\text{DC}} = 0.6 + (1 - 0.5)0.4 = 0.70$$

where we have taken $\eta_{\text{DC}} = 0.5$ and $\eta_{\text{TH}} = 0.4$.

With thermal cycle advanced to higher temperatures and better direct converters, it is completely plausible that:

$$\eta_{\text{DC}} = 0.6 + (1 - 0.5)0.55 = 0.84.$$

This is really a ternary cycle combining, for example, a relatively high quality DC [4.8], a potassum cycle intermed¹ stage and a "steam bottoming stage.

In the blanket discussed in Section 2, the neutron kinetic energy (~ 80% of the total thermonuclear reaction energy) is converted to thermal energy and DC conversion is not possible. The analog to the DC converter that permits the blanket to be more effective is blanket energy multiplication (M) so that the overall blanket energy recovery efficiency for the neutron energy is:

$$\eta_{\text{BH}} = \eta_{\text{BH}} + M$$

where M is the energy enhancement due to exothermic reactions such as $n(\text{Li-7})\text{He-3} \rightarrow \text{He-4}$. In this case, M would be:

$$M = \frac{14.1 + 5.8}{14.1} = 1.34.$$

With other (n, 2n) reactions, the value of M can be as high as 1.9 for a completely enveloping blanket and 1.7 for a blanket with suitable penetrations for injectors, etc. [4.9]. Thus, with a modest thermal efficiency of 0.40, the blanket performance could be:

$$\eta_{\text{BH}} = 0.40 \times 1.7 = .68$$

this energy enhancement is also a necessary condition for breakeven with low η systems (i.e., in order to obtain a sufficiently high value of the overall system efficiency η_{sys} where

$$\eta_{\text{sys}} = \frac{1 + \eta_{\text{inj}} + \eta_{\text{heat}}}{1 + \eta_{\text{inj}}}$$

with more or less simple illustrations, it can be seen that the processing of the blanket power and the circulating power will require a substantial amount of heat transfer ingenuity. Certainly the energy will have to be lost outside the thermal efficiency, and high thermal efficiency. If the present plasma investigations into mirror machines are a major variable with higher η_{inj} , it is a fact that the η_{inj} may improve [4.13, 4.14]. In addition, there would probably a new generation of Mirror reactors, such as a "compact" or "deuterium" in energy recovery efficiency from the current η_{inj} [4.15].

A schematic of a Mirror reactor with emphasis on the first wall of the system is shown in Fig. 4.1. In this, the bulk plasma is negative ions. The use of divertors is not a typical of systems where the first wall energy loss is greater than 10% and is not unique to Mirror machines. Similar systems, such as the Westinghouse model, utilize a plasma heating at injection energies as high as 100 keV. The use of magnetic cone (one end of a neutral cone accelerator) and a stripping coil of neutralization to the basic injector system provides a safe regime where heat transfer must be considered.

In similar systems, Fig. 4.2, shows an operating system at a typical Tokamak reactor where the plasma is composed of "well-confined" ions.

It can be seen that for this model there is a necessary long heating period to raise the plasma temperature to a point where internal heating of the plasma by the fusion alpha-particle can take over. This plasma heating is done by injection of streams of energetic neutrals at an appropriate energy and total power (exactly the same as injection into the Mirror machine would be accomplished). Thus, as regards the injector phase in either "poorly confined" or "well confined" plasmas, the heat transfer problems are quantitatively the same; that is, injectors in both systems are subjected to the same energy loss requirements, to high current density beams, to the heat transfer and activation effects of the strong neutron flux emanating from the nearby plasma, to the effects of high magnetic fields on pumping of any electrically conducting coolant, to the remote handling and maintenance problem, to highly limited visual access and to other hostile environmental considerations. However, the steady-state, continuous energy injection as is required by Mirror machines compared to the short energy injection time of 10 sec out of 90 min suggested for the Tokamak reactor makes mirror heat transfer problems substantially more difficult. It is not unreasonable to suppose, however, (and most researchers now take this position) that as the first wall surface effects on plasma cooling are fully taken into account, the burn period will decrease from the hoped for a 90 min cycle to a time perhaps not substantially greater than the 20 sec heating period [4.13, 4.14]. In that case,

the magnitude of heat transfer problems for the injectors in both the Mirror and the Tokamak would be about the same. Some examples of injector heat transfer problems will be discussed in Section 4.4.

With all plasmas, there is an inevitable interaction between the plasma and the first wall. Actually, there is substantially more plasma-wall interaction with "well confined" than "poorly confined" plasmas. In the latter, the dominant process is leakage out the ends and, hence, the low Q. The "well confined" plasma is not confined perfectly and high energy neutrals diffuse to the walls. These neutrals dislodge atoms of first wall material or dislodge adsorbed gas from the surface. The impurities impinge on the plasma, become ionized and cause energy loss by radiat^{on} which can be sufficiently high to quench the plasma or markedly affect its lifetime. In an attempt to minimize these effects, a divertor is introduced. A representative divertor is shown in Fig. 4.3. The divertor consists of a coil, magnetically opposed to the confining field, which diverts the flux lines adjacent to the wall out of the machine while allowing the central flux to pass through. Thus, particles diffusing out of the plasma toward the wall preferentially follow the escaping flux lines out of the system without reaching the first wall [4.15]. In addition, neutrals sputtered off the wall by other causes (perhaps neutron sputtering) [4.16] are ionized at the plasma surface and diverted.

The divertor must be a very effective particle "shunt" in pumping the charged particles along the diverted field lines. Thus, in principle it is similar to a direct converter and could be used for that purpose if the quantity of energy diverted warranted direct conversion. The extracted ions are pumped to a region external to the main toroidal volume where they are collected by burial in solid or liquid targets and subsequently recovered for reinjection. Since the particles have substantial energy on impact into the target, a heat transfer problem is created. The divertor must have an efficiency associated with its operation of the order 90%; consequently, there remains some plasma-wall interaction. To alleviate this problem further low Z first walls have been proposed such as the carbon curtain in UMK-1. This may introduce a heat transfer problem, methane gas evolution, etc. The basic physics difference between the Mirror machine direct converter and the Tokamak divertor is that the divertor is purposely introduced to inhibit plasma-first wall interaction. It diverts particles which diffuse out in coordinate space while the direct converter recovers the energy of particles that diffuse out in velocity space towards the mirrors and which cannot be contained. We will discuss the heat transfer problems of direct converters, divertors and injectors in the following three sections.

4.2 Direct Convertors. A representative direct converter is shown in Fig. 4.5. The process of conversion of charged particle energy to electrical energy takes place in a sequence of four steps:

- 1) Expansion
- 2) Charge separation
- 3) Deceleration and collection
- 4) Conversion to a common potential

As suggested in Fig. 4.5, the reaction products

and unburned fuel escaping from the mirrors at low ion density (typically $10^8/\text{cm}^3$) would be further expanded into a larger chamber where the density would be reduced to about $10^6/\text{cm}^3$. The expansion process would be done adiabatically similar to expansion in a nozzle. Adiabatically, in fusion terminology, means that the rate of change in magnetic field with distance is sufficiently slow so that particles still stay on field lines. Free expansion, e.g., without the use of supplementary field windings, is implied in the figure and the field decrease is from ~ 16 T at the reactor mirror to roughly 1/300 of that value at the end of the expander. The effect of this expansion is to reduce to an acceptable level the value of the power flux (to $\sim 100 \text{ W/cm}^2$) entering the collector region so that heat transfer can be accommodated and acceptably low thermionic emission from collector elements is produced. The charged particles' rotational energy is also converted to translational energy. At the end of this expander field, the electrons are collected by the action of a negative potential grid reflecting them to a collector at ground-potential grid. The positive ions which contain the bulk of the energy compared to the electrons yield this energy to a series of collectors. Each collector is kept at a different electrical potential. The potential of the first collector being lower than the average potential of the particles and the last collector being higher than the average particle potential. The ions, because of their $> 99\%$ translational energy after expansion, enter the collector region in a highly directed stream. Initially, the ions are directed at a slight angle to the applied uniform electric field. Therefore, the trajectories are parabolic, as is shown in Fig. 4.6. The incoming ion trajectories are aligned with the collector plates and thus see an almost completely transparent grid. However, after the ions have lost their forward motion, they are turned by the higher potential end see an opaque grid on their return path. The ions that hit a particular collector produce a current at the voltage of that collector stage. Since collection efficiency is less than 1, the ions have residual kinetic energy on impact which is converted to thermal energy which must be recovered in a suitable thermodynamic cycle.

Figure 4.7 shows a heat transfer model of a three-stage direct converter based on the Venetian Blind collector concept [4.17]. Other D.C. converters have been suggested but the Venetian Blind Direct Converter (V.B.D.C.) will serve to illustrate the general heat transfer problems [4.18]. The precision of alignment of collector plates in the V.B.D.C. creates one of the most severe problems of heat transfer. This converter, as was indicated in Fig. 4.5, is at a distance typically 50 to 75 metres from the reactor plasma center, and consequently, the magnetic fields are very low. The direct converter is not subjected to neutron damage of any consequence. However, it is subjected to sputtering and surface erosion from the particle flux and this primarily sets the life expectancy of its components. In principle, the direct converter has better access for repair and maintenance than does either the blanket or the injector and perhaps the divertor also. Unfortunately, the V.B.D.C. has to be a precision instrument to be efficient, and alignment of collectors, grids, etc. must be done with a preci-

sion measured in tenths of millimetres in a system whose major dimensions are typically measured in tens of metres. To compound the alignment problem and the heat transfer problem, temperatures in the converter unit range from ~ 1800 K at the grid wires to 4 K at the cryogenic pumping panel located only about 3 or 4 metres away. Virtually no thermal communication can be permitted between grid wires and cryopanels or between collectors and cryopanels.

Following a charged particle through the system will be instructive in appreciating the magnitude of the heat transfer problems. First, the power flux into the collector array (100 W/cm^2 in Fig. 4.7) is limited by thermionic emission of electrons from the negative grid. Each electron emitted and then collected by a collector plate cancels the charge of an ion and reduces collection efficiency. The influence of the negative grid on efficiency is approximately:

$$\eta_{DC} = \eta_{DC0} [1 - 1.7(1 - T)]$$

Here T is the transmission factor, or effectively, the transparency of the grid array to the ions, and η_{DC0} is the efficiency without the effect of thermionic emission. A typical (and probably necessary) value of $(1 - T)$ is ≤ 0.01 . Other electrical constraints coupled with limits on T result in grid wires having diameters of only a few millimetres. The span of an individual wire by comparison may have to be three metres or more. The high temperatures on the grids are a necessary evil due to these physical dimensions, because the wires must probably be radiation cooled. It is only under unique circumstances that the long, small diameter wires could be convectively cooled. The grid array will almost certainly be in the form of an interlocking net rather than a series of parallel, independent wires, so that wire breakage becomes a much less severe problem. Figure 4.8 shows the combined effect of emissivity and work function on direct conversion efficiency as influenced by the grid wires. It can be seen from the set of curves that what is required in addition to fundamental high temperature creep strength and reliability for time periods like a year is a material that has a combination of both high work function and high emissivity. A rhodium-coated tungsten wire at first glance seems best based on the curves of Fig. 4.8. However, if collector plates are made of carbon, as is generally proposed, then sputtered carbon atoms will deposit on the grids and they will then have the emissivity and work function corresponding to carbon. Furthermore, if tungsten were to be used as the basic structure of the grid, it would take little time (a few hours) to convert it to the very brittle tungsten carbide, WC. So it may be necessary to use carbon fibers for the grids if a carbon plate system is used. On the other hand, changing the collectors to a refractory metal grid would permit use of a refractory metal grid.

Figure 4.9 shows thermionic emission as a function of temperature for three selected materials. The example chosen shows that a 1% power loss with $\eta_{INC} = 100 \text{ W/cm}^2$ corresponds to a maximum allowable grid wire temperature of 1680 K if tungsten

cerbide wire or carbon filaments are used, 1920 K if tungsten is used and 2070 K for rhenium wire. For the particular radiation characteristics of a typical expander and collector plate system, the actual grid wire temperatures reached in steady-state are shown by the triangles. It can be seen that only the rhenium-coated wires can limit the thermionic emission loss to 15 or less.

Figure 4.9 also implies that the sensitivity to the incident flux is very great. If, for whatever cause, the flux were $\sim 190 \text{ W/cm}^2$ instead of 120 W/cm^2 , the loss by thermionic emission would have increased in order of magnitude independent of what material had been selected. Because thermionic emission is so temperature sensitive, it is perhaps desirable to consider flat or elliptical cross-sections instead of round wires for the grids. If the ribbons could be aligned with the ion stream for minimum losses, the additional radiating surface area would decrease the temperature and, hence, the emission at a faster rate than the total thermionic emission increased with area. From a practical viewpoint, it would seem doubtful if this alignment could be accomplished or retained for long time periods.

The function of the grids is to reflect and then capture electrons while allowing the ions to proceed to the collector for energy recovery. Once the electrons are captured, the neutrality of the plasma is lost and space charge effects come into play, and can limit the ion current to the collectors. The electric field due to space charge must be kept small enough so that the ions are not prevented from reaching the proper electrode. The space charge determines the **maximum** spacing, d_4 , between successive stages of collection as indicated in Fig. 4.10. It can be shown that [4.19]:

$$d^2 \propto \frac{W^{5/2}}{q}$$

where W = ion energy and q is the incident flux. Computer calculations with an approximation to the expected energy distribution show that for d^2 ions with $W = 200 \text{ keV}$ and $q = 100 \text{ W/cm}^2$, the maximum spacing from the negative grid to the first collector stage would be approximately one metre and the distance from first to second stage approximately 0.8 metre.

For a given collector stage, the separation between plates, h , must be $< d/4$ to prevent severe distortion of the electric field at the leading and trailing edges of the collector plates. The plate thickness, δ , must be kept small to limit interception of the ions to a small percentage. The value of δ should be of the order of .01 h or perhaps .02 h. The effect of δ on collection efficiency is approximately:

$$\eta_{DC} = \eta_{DC0} (1 - 6/3h)$$

A consistent example would require a d of about one metre, h about 0.25 metres, and δ only 2.5 millimetres to perhaps 5 millimetres.

The width of the collector plate must be $\sim 2.5 \text{ h}$

for reasons related to collection efficiency. It should be noted that these illustrative values are near the upper limits and that from a physics standpoint, it would be better if d , h , and δ were all smaller.

The length of an individual collector plate may be from 3 to 12 metres depending on how the total array is modularized and is generally independent of collector physics. These dimensions preclude convective cooling for the first and second stage collectors and radiation cooling must be used as was required of the grid wires. In the model suggested in Fig. 4.7, it was assumed that the first stage radiates to the 1000 K surface of the remote expander walls and achieves a temperature of $\sim 1500 \text{ K}$ by radiative energy balance. The second stage is assumed to be held at the same temperature as the first and, therefore, there is no heat exchange between these two stages. Stage 2 radiates only to stage 3. Stage 3 fortunately may be convectively cooled with helium at $\sim 1000 \text{ K}$. This convection cooling is possible because the ions that arrive at the third or final stage can be collected by direct impact and do not need the parabolic trajectory and the high collector transparency; in addition, the plate thicknesses, δ , can be relatively large. However, some spacing has to be inserted between third stage collector plates so that gas vacuum pumping is impeded as little as possible.

If all stages were to be radiation cooled or more than 3 stages were used, then higher temperatures would have to be acceptable on the interior stages. Otherwise, i.e., the incident flux, would have to be decreased if temperatures were already at their maximum. To decrease q , more magnetic expansion is necessary and the physical size of the expander would increase.

Several choices of coolant fluids are possible for last stage cooling, but it must be recognized that the collectors are all at potentials of 100 to 200 kilovolts above ground. Therefore, even though they are out of the high B field region, conducting coolants such as potassium or sodium cannot be used, even though thermodynamically they might be advantageous. In fact, because of the almost extreme need to conserve efficiency because of low q , the power loss to ground for any coolant must be a small fraction of one percent. This leads to the choice of helium as one of the more promising third-stage coolants.

Assuming uniform distribution of the 100 W/cm^2 between stages, the energy flux that stage 3 must handle is $\sim 46 \text{ W/cm}^2$ total. Approximately 40% of this is thermal energy ($\sim 18 \text{ W/cm}^2$) for a direct converter net efficiency of 60%. The first set of chevron baffles for the cryopanels shown in Fig. 4.7 represent a possible preheat section for the third stage or at least a necessary thermal barrier. There is some incentive for the incoming coolant to pass through a preheat stage. This stage could serve to shield the 77° liquid nitrogen panels from the 1000 K third-stage collector. The penalty in dumping energy q_A into the liquid nitrogen panel is:

$$q_A \times \frac{\text{ACTUAL WORK REQ'D TO LIQUIFY } N_2}{N_2 \text{ LATENT HEAT OF VAPORIZATION}}$$

The latent heat of vaporization is $\sim 2 \times 10^5$ J/kg. The work to liquify nitrogen is illustrated in Table 4.1 from p. 17 of "Cryogenic Engineering".

If we take the mean value of the four more optimistic lower values for work required to liquify N₂, the penalty is roughly

$$\frac{3.4 \times 10^6}{2 \times 10^5} = 17 \text{ watts of work per watt input}$$

If no preheater or shields were used for thermal insulation, then the heat exchange between the liquid nitrogen cooled chevrons (at T_N = 77 K), and the relatively hot third-stage collector plates (at T_H = 1000 K) would be:

$$\begin{aligned} q_{H-N} &= \frac{\sigma(T_H^4 - T_N^4)}{1/\epsilon_H + 1/\epsilon_N - 1} \\ &= \frac{5.67 \left[\left(\frac{1000}{77} \right)^4 - \left(\frac{77}{303} \right)^4 \right]}{1/1.5 + 1/1.1 - 1} = 0.553 \text{ W/cm}^2 \end{aligned}$$

and the work required would be $17 \times 0.553 = 9.3$ W/cm². This is almost 10% of the power into the converter and about 30% of the electrical power output. Consequently, an intervening surface is efficiently required.

If the energy is radiated from the 1000 K third-stage collector to this intervening surface used as a 300 K preheater, then by definition, that energy is recovered. The radiant loss from the preheater to the N₂ panel would then only be:

$$\begin{aligned} q &= \frac{5.67 \left[\left(\frac{300}{77} \right)^4 - \left(\frac{77}{1000} \right)^4 \right]}{17.8 + 17.1 - 1} \\ &= .0045 \text{ W/cm}^2 \end{aligned}$$

The preheater thus has an effectiveness of $0.553/0.0045 = 123$. So the work required to re-liquify the N₂ is reduced to $9.4/123 = .076$ W/cm².

In principle, the preheater concept works well. There is a penalty to be assessed, however, in that some pumping power is required in pumping the coolant through the preheater tubing. This must be a small penalty to be acceptable. Another penalty is due to the increased impedance from the collector region to the cryo-pans. If this were to result in higher background neutral gas pressures, a loss in direct conversion efficiency would result due to ion charge exchange collisions.

In lieu of the preheater, it is possible to substitute a set of N thermal shields. To retain the same effectiveness of 123, the number of shields required is 124. This is not necessarily a large number as far as first cost goes. However, extremely high surface areas are introduced and the neutral gas pumping problem (the D₂ and T₂ pumping) is probably aggravated both by the

large area and by the higher impedance. The gas pumping, incidentally, is far from a trivial problem and makes the overall heat transfer problem more complicated. The pumping load is determined from the total flux of incoming ions. For this example:

$$\frac{P_w}{W = 6 \times 10^{-19}} = \frac{20 \times 10^6}{300 \times 10^5 \times 6 \times 10^{-19}}$$

$$= 3.3 \times 10^{20} \text{ particles/sec}$$

To effectively pump this quantity of hydrogen type gas, cryogenic pumping has been assumed. The cryogenic panels operating at liquid helium temperatures of ~ 4 K must be isolated from ambient temperatures and, thus, are surrounded by the 77 K nitrogen panels. The penalty paid for energy deposition into the liquid helium is much more severe than that into nitrogen. Estimates for this penalty range from 300 to 1000 watts required to reliquefy the helium for each watt of input.

As can be seen from the above example, tremendous amount of engineering work remains to be done on direct converters. The V.B.D.C. is extremely interesting from a physics and energy conversion standpoint. However, it has been shown to have some interrelated structural/heat transfer problems that may be extremely difficult to solve within the narrow allowable limits on losses in efficiency that are tolerable with low Q systems.

4.3 Divertors. Heat transfer work on divertors has not, as yet, been very extensive. There is a series of twelve papers compiled by Bill Cough, ABC in 1971 which although somewhat dated, provides good historical perspective on the divertor problem [4.21]. None of these papers, however, has specific information on heat transfer.

In reviewing the papers from the second IAEA workshop held at the Culham Laboratory, UK in January, 1974, it was also to be noted that of the 45 papers presented, none dealt with divertor heat transfer [4.21]. This workshop was primarily concerned with fusion reactor design problems but included reasonably strong phys's input. Perhaps the most important physics presented at the workshop was that having to do with the likely effect of impurities or the plasma - an effect possibly so strong that the operating time of a quasi-steady-state Tokamak reactor with a hoped for duty cycle of 90 minutes would degenerate to times measured in tens of seconds. These plasma-wall interaction data have been generally known to the physicists, but unfortunately they had not been factored into the engineering design considerations. It was at this meeting, therefore, that the divertor took a sudden jump in importance as a primary element in toroidal reactor design. It also took a large jump at this time in the quantity of power it was likely to handle. This was probably the first recognition that some new and difficult heat transfer problems were likely to appear in this upgraded divertor.

In the Princeton reference design 1, published

In August of 1974 (actually prepared for the Culham meeting the previous January), some minor attention was given to divertor heat transfer [4.11]. As indicated in Fig. 4.12, the divertor walls in that model were cooled with helium having a low inlet temperature (16°C) and a fairly substantial outlet temperature (153°C). The exit temperature implies that this energy could be recovered in a thermodynamic cycle although the power in the divertor region is only about 7% of the total. Also, the average power flux falling on the divertor wall was expected to be only 120 W/cm^2 , a relatively small flux requiring only routine heat transfer treatment.

In the Wisconsin reference design, KWAk-II, published in late 1975, it was suggested that the hydrogen isotopes escaping from the plasma to the divertor could be recovered in a flowing liquid lithium sheet as indicated in Figs. 4.12 and 4.13. The average thermal load on this lithium cascade was given as 781 W/cm^2 . The energy is distributed approximately exponentially along the flow path according to their equation:

$$Q = 15 \exp\left(-\frac{x}{15.5}\right) (\text{MW/m}^2)$$

It was not stated what range of x values were assignable to x in the equation, but if it may reasonably be assumed that x is a length dimension starting from zero, then the maximum thermal flux would be 1800 W/cm^2 . This high flux certainly provides an extremely difficult heat transfer problem particularly with unconfined free falling lithium where surface evaporation would seem severe. Additionally, the lithium flow must be approximately normal to a relatively high magnetic field and it is possible that the flow will be disturbed by MHD effects.

The factor of 100 difference in the estimated thermal flux between the Princeton design and Wisconsin design for two machines that are basically similar provides an indication of the uncertainty of understanding of energy fluxes and heat transfer in divertors. How severe the heat transfer problem may be is really not yet known.

The recent IEEE meeting held in San Diego in the fall of 1975 had several papers on divertor heat transfer that are worth review [4.22]. They were not available at the time of this writing.

There will also be information forthcoming as machines such as the Princeton TFR go into the design state.

4.5 Injectors. The work on injectors has been largely dedicated to a development program to produce increasingly higher current densities and quasi-continuous injection. Injectors proposed in various conceptual design studies have not been discussed in any detail with the possible exception of an injector system for a Mirror reactor [4.23]. The work to date has been limited to on-going experiments requiring injectors or next generation machines [4.24, 4.25].

The principle of operation of injectors using either positive ions or negative ions is illustrated in Fig. 4.14. Figure 4.15 shows the neutralization efficiency as a function of energy

for D^+ and D^- .

The goals of the injector development program are as follows:

- 1) High current density at the "window" into the plasma.
- 2) High energy to penetrate the plasma.
- 3) Low gas influx into the thermonuclear plasma.
- 4) Direct energy recovery of the non-neutralized ions followed by thermal recovery.
- 5) Quasi-DC injection.
- 6) High charge exchange efficiency in the neutralization cell.

By examining this list, it can be seen that each of the six goals of the development program will produce its own particular heat transfer problems and that the severity of the problems will often increase in proportion to the success in improving the injectors. For example, as higher and higher current densities are achieved, two main heat transfer problems arise: (a) The divergence of the beam due to space charge effects will require that the "window" through which the neutral particles are injected be made somewhat larger to keep the neutral beam impingement on the frame of the "window" to acceptable levels within the constraints imposed by erosion and heat flux. (b) Some fraction of the high current density beam will not be trapped by ionization in the plasma and will deposit energy on the far wall or into a beam dump.

Should the plasma be lost or go unstable, then all the beam energy must be absorbed by the wall or the beam dump. As higher energies are achieved to get better penetration, then the quantity of energy that completely penetrates also increases and coupled with (b) creates a thermal flux on the wall that could be extremely high (perhaps as high as 10 kW/cm^2 as discussed in Section 3). The complexity of direct energy recovery of the non-neutralized ions increases with higher current densities and higher voltages. Estimates of the residual thermal flux on the collector plates after direct conversion range as high as 10 kW/cm^2 for short pulse times ($\sim 500\text{ ms}$) for a model being worked on at LBL in Berkeley for application to the TFR [4.26]. Quasi-DC injection will make it necessary to provide for cooling of accelerator stages and beam optical components.

The achievements to date on beam development are:

Lab	Total Current	Energy	Current Density	Pulse Time
LBL	14 amp	40 keV	.25 A/cm ²	200-500 ms
ORNL	16 amp	50 keV	.25 A/cm ²	500 ms

These achievements, accomplished over a time period of about 5 years starting from a beam source with a total current of only $\sim 0.1\text{ A}$ at 20 keV, have come in part from an effort to have a neutral beam injection system ready for TFR (Toroidal Fusion Test Reactor) when this machine is built.

The TFR Tokamak to be built by the Princeton Plasma Physics Laboratory (PPPL) is by far the

largest and most complex U.S. fusion experiment planned for this decade. The deuterium neutral beam injection system required for heating the tritium plasma, and produce a reactor-like D-T reaction rate in the hot plasma, require neutral beam injector performance which considerably exceeds the present state of development.

The performance requirements of the neutral beam injection system for TFR relevant to heat transfer are as follows:

1) Beam Specifications:

Accelerator Power = 80 MW
Accelerator Voltage = 120 KV (This may be increased to 150 KV)
Total Accelerator Current = 672 A
12 sources (46 A each)
Pulse Duration = 5.0 ms

2) Beam Lines:

7 beam lines, with provision for 2 more
7 sources per beam line
Beam lines will be aligned with one coil gap between adjacent beam lines.

3) Beam Line Dimensions:

Approximately 9 m from torus to far end of vector system.

4) Attachment Points:

A) 70 cm high - inside clearance
B) 40 cm projection width: The duct will be wider than this where possible
C) The power density deposited on walls should be less than $P = V x .01 A/cm^2 = 1.2 kW/cm^2$

5) Beam Dump and Calorimeter:

These will have to be the subject of a Research Task [4.27].

SECTION 5. SUPERCONDUCTING HEAT TRANSFER PROBLEMS

5.1. General. The prime role that superconductors are expected to play in fusion reactors is to produce and maintain the magnetic fields which confine the hot plasma. The power requirements of conventional magnets would be so enormous that it is almost universally acknowledged that superconductors must be used to obtain a useful net energy output from a commercial reactor.

Some confinement systems also require their use for other roles --- in the Theta-Pinch system for energy storage, and in the Tokamak system for start-up, stabilization and divertor windings. It is also possible that these other requirements for the Tokamak system will also need superconducting energy storage.

A whole range of heat-transfer problems is introduced by the fact that a superconductor only retains its superconducting properties under certain rigid conditions, one of which being that its temperature does not exceed a critical value. The particular value is dependent on a number of other factors such as the type of superconductor, the ambient field strength and direction, and the current density. For most applications the temperature must be kept well below 10 K, thus necessitating use of the cryogenic properties of liquid or gaseous helium.

Of all the criteria that must be met and sustained, that of critical temperature is probably the most difficult to achieve and guarantee,

particularly as systems grow in size, energy and complexity. The penalties for exceeding it also grow with these factors. Only a slight increase, a small fraction of 1 K, can cause an immediate transition from the superconducting to the "normal" state. Should this occur for any reason, the conductor, which is operating at a current density well in excess of that normally used in conventional copper conductor, suddenly exhibits a very high resistance comparable to that of stainless steel, for instance. At the low operating temperature, the specific heat of solid materials is almost negligible -- it approaches zero at zero K. This means, firstly, that only a very small heat transient will cause the critical temperature to be exceeded. In this event, the current continues to flow because it is in a large inductive circuit and the stored energy begins to be dissipated rapidly in this highly resistive "normal" part of the coil. Thus, unless special precautions are taken, melting temperatures and electrical breakdown voltages between turns and layers are rapidly reached with disastrous results to the coil.

This section will discuss how these problems affect the design of superconducting systems and fusion reactors together with the means and extent to which they are being solved and the directions in which further research and development must be pursued.

5.2. Requirements of Different Magnetic Systems. It is impossible to cover all aspects of all possible configurations in this paper. It is, therefore, proposed only to discuss the more important aspects of the three most popular types, Tokamaks, Mirrors, and Theta-Pinches.

5.2.1. Tokamaks. Of these three systems, the Tokamak, originating in the U.S.S.R., is currently the most popular geometry in all of the major centers of fusion research. The toroidal field for such a reactor, generated by 70 to 30 coils (see Fig. 1.2) up to 10 metres in diameter equally spaced around the major diameter of the machine, also represents the largest energy store of all the systems, about 10^5 MJ or 30 MWh.

In operation, one of the first major heat-transfer tasks to be undertaken is to cool the whole mass of the superconducting coils and force-restraining structure from room temperature to about 4 K. The mass of the toroidal system for UWAK-II [5.1], for example, including the low-temperature structure, is in the region of 4000 Mt. This cooling process must not only be carried out in a reasonably short time, but great care must be taken to limit differential contraction to safe values. This is no easy task when the coefficients of thermal expansion of the various materials can vary by orders of magnitude and the cooling characteristics of the cooling media change by orders of magnitude as the temperature falls. However, these problems are now becoming reasonably well understood and low temperature data on materials is being continually up-dated.

Having cooled the system to its operating temperature, the refrigeration system must continue to maintain that temperature against the operational heat leaks into the low temperature system. The major sources of heat are:

- Thermal radiation from room temperature.

This heat input is normally reduced by the use of either shields held at intermediate temperature using a higher temperature coolant such as liquid nitrogen or by many layers of superinsulation.

b) Heat conducted through a support structure designed to both support the weight of the low temperature structure and to resist any forces developed between the coils and the room-temperature structure. In the case of pulse forces, particularly for those occurring only under fault conditions, the steady-state heat leak can be reduced significantly by introducing small vacuum gaps or poor thermal contacts in the supports which only close up, giving an increased heat leak during the transient force conditions.

c) There will be losses in the main current leads to the coils. There are both heat conduction losses and Joule losses. Usually the leads are forced and the heat leak minimized by passing cold helium gas from the coil chamber through the lead. The duty cycle, the method of cooling the coil, and a number of other factors all influence the optimization calculations of the lead so that each case must be considered on its own merits. However, in general terms, an economical lead is one in which the temperature of the gas leaving the lead is close to that of room temperature since it has absorbed little useful enthalpy.

13. While superconductors exhibit zero resistance under D.C. conditions, this is not so when either the current or ambient field are varying with time. Thus, the superconducting diameters in the pulsed poloidal windings of T-karok will generate eddy current and hysteresis losses. Even the D.C. toroidal field winding will exhibit losses by virtue of being subjected to pulsed fields from the plasma current and poloidal field and "vector" windings. Similarly, eddy current losses will be generated in the copper or aluminum in which the superconducting filaments are embedded which can have a profound effect on the construction of the conductor and indeed upon the overall efficiency of the reactor. This is because the efficiency of refrigerators falls rapidly as the output temperature is reduced, although, fortunately it increases with plant size and capacity. For example, Ref. 5.1 quotes the total heat leak for their reactor as 15.5 KW at 4 K and estimates that this will require a continuous room temperature power of 4.60 MW.

Effects of thermonuclear neutrons penetrating the shield and entering the superconducting system must also be considered. The thickness and composition of the shield must be such that the thermal energy released in the 4 K system, where 1 watt at 4 K requires about 300 watts of refrigerator power, does not have too great an effect on the overall efficiency of the reactor. McCracken and Bliv [5.2] have considered this problem together with radiation damage effects. The conclusions from their study can be summarized briefly as follows.

a) The neutron heating will affect the refrigeration load and must, therefore, be limited to a reasonable value. In addition to the

thermal blanket, a shield thickness of about 55 cm would be required to limit the refrigeration load to 1% of the station thermal output.

b) The limit imposed by (a) is such that the conductor temperature rise due to radiation will not be significant.

c) Some degradation of the superconductor performance can be expected as a result of radiation damage but this is not expected to exceed 10%.

d) The resistivity of the stabilizer will also be increased by radiation damage. Almost complete recovery in the case of aluminum and about 80% recovery for copper can be obtained by cycling the system to room temperature once every year or so.

Radiation effects on the magnets, particularly as postulated by later design studies, do not, therefore, appear to present major problems in the way of damage or heat transfer when sufficiently thick blankets and shields are employed.

The reliability of present-day, small, 4 K refrigeration systems, would certainly not meet the requirements of a commercial power-producing plant. Fortunately again, experience is showing that reliability is also improving with size. However, it is significant that ten 3-kW refrigeration units are included in the UNKAKU-III proposal, seven in operation and three held in reserve.

The difficulties of insuring that all of the conductor is below the critical temperature whenever the machine is operational means that at least the first generation of Tokamak reactors will probably use "cryostatic" stabilization. This is in spite of the many disadvantages which accompany this mode of operation. Perhaps the most serious of these disadvantages is the presence of the stabilizing "normal" material which may well occupy more than 20 times the space needed for the superconductor alone.

The principle of "cryostatic" stabilization is to provide an alternative path for the current when some transient phenomenon (e.g., heat generated by friction as conductors move relative to each other under the influence of electro-magnetic forces) causes a local region of the superconductor to go "normal". Cryostatic stabilization requires that the cooling of the "normal" region of conductor be sufficient to allow the conductor temperature to return to less than its critical value even though additional heat is now being generated by the current flowing in the stabilizing material. Thus, in addition to its superconducting properties, desirable features of the conductor are low electrical resistance, high thermal conductivity, large cooling surfaces and good heat-transfer characteristics to the coolant. It should also be noted that the conductor current rating and, therefore the conductor cross-sectional area, increase for a variety of reasons as the system size and stored energy increase. Unless a wide, thin strip conductor can be used, this means that the ratio of cooling surface to conductor size decreases as the machine size grows, thus making the stability criterion increasingly more difficult to achieve.

The largest superconducting magnets yet built have been bubble-chamber magnets for high energy

physics research and all have been "cryostatically" stabilized [5.3]. They are similar in that wide strip conductor is used in disc coils, but as coil technology has developed, filament twisting to avoid circulating currents and flux jumps has been incorporated. Also, as experience has been gained, the heat flux from the conductor to the helium will all the current flowing in the copper, has been increased from 0.1 to approximately 0.4 w/cm².

Although these magnets provide much valuable experience, the requirements of fusion magnets are more exacting. Higher current densities, higher fields, ruled fields, more complex geometries and much greater stored energy will all be required. [e.g., The largest "bubble-chamber" magnet, at CERN, stores 72 MJ while a typical Tokamak might have about 10 MJ stored in the toroidal field.]

The bubble-chamber magnets referred to above have all been operated with the conductor fully immersed in liquid helium at atmospheric pressure (i.e., pool boiling). There are, however, alternative modes in which helium can be used as the coolant. Forced convective two-phase flow, forced convective single-phase flow, and saturated or unsaturated Helium-II are some of the possibilities. Reference 5.1 discusses and reviews each of these in some detail.

The two main contenders being considered at this stage for reactor coils are pool boiling and forced convective single-phase flow.

The conductor shown in Fig. 5.1 and close variants on it are being considered for the Lawrence Livermore Laboratory's next plasma physics machine proposal, UNMAK-II, and for the poloidal field windings in the UNMAK-III conceptual design study. It is virtually impossible to wind the large Yin-Yang coils for the UNX machine with wide strip conductors. To enable it to be wound satisfactorily, the conductor must be square or if it is rectangular, its aspect ratio must be small. Since the square shape has a poor surface to volume ratio, it is proposed to increase the cooling surface by including internal cooling channels. The conductor comprises four elements soldered together. All of the superconducting filaments are contained in one element, the remaining three elements providing the stabilizing copper and cooling surface. The cooling channels between the elements will be at an angle of about 45 degrees so that when combined with about 50% of the external surface available for cooling, the heat transfer characteristics should be largely independent of conductor orientation (see Fig. 5.1). It is proposed to carry out heat transfer measurements on this type of conductor in the near future.

The "Omega" magnet at CERN [5.5] is the only magnet of any size which has yet been built with hollow conductors and forced convection single-phase coolant flow. However, the system is presently being studied by M.I.T. [5.6] on subcontract to ORNL with a view to using it for Tokamak toroidal coils. Fig. 5.2 shows the general design principle of the conductor. Fluid is forced through the tube which contains many small diameter strands. The large number of

small diameter strands presents a large surface for cooling and coil construction may be simplified since the coolant is contained inside the conductor. However, many questions remain to be answered with such a system before it can be considered to be developed to the degree of reliability necessary for a reactor.

It is clear that considerable research and development is still required in the area of heat transfer to helium for cryostatic stabilization purposes.

5.2.2 Mirror Machines. Many of the aspects previously discussed in relation to the Tokamak also apply to the other types of magnetic confinement systems. Further comments are therefore limited to areas of significant difference.

On the credit side, the Mirror reactor, as presently envisaged, requires only a D.C. magnetic field. While the most important benefit which may be derived from this is probably associated with mechanical fatigue problems, the absence of A.C. or pulse losses which permits a less complex conductor and low-temperature structure, is a welcome simplification.

The present concept of the main confining field of a Mirror reactor consists of a pair of identical Yin-Yang coils which are wound separately and are in no way interlinked (Fig. 1.1). In contrast to this, the poloidal field windings, (start-up, stabilizer and divertor) for Tokamak machines must either be wound inside the toroidal field coils, thus linking them and causing many manufacturing and cryogenic problems, or they must all be situated outside the toroidal field coils. In the latter case, as shown in UNMAK-I, the resulting increase in size and stored energy become almost un-tenable.

The Yin-Yang shape of the mirror coils is clearly on the debit side. Circular coils or "D"-shaped "constant-tension" coils for Tokamaks are themselves capable of absorbing much of the magnetic force although some additional strengthening is required. In contrast, very little tensile strength can be wound into a Yin-Yang geometry coil and the majority of the electromagnetic force will accumulate through the coil and as a first approximation can be represented by the full magnetic pressure on the coil case. The coil cases and inter-coil structure must, therefore, be designed to take the whole of this force without exceeding the permissible deflections and conductor strain. This situation also implies that the conductor bundle (i.e. complete winding) must be capable of transmitting this pressure to the coil case. At 8 T, the pressure is approximately 26 Mpa (3,700 psi). If half of the conductor surface is to be available as cooling surface, leaving only half for load-bearing, the local stress is close to the allowable stress of annealed copper. In a reactor, the desired field is in the region of 16 T [5.7] which will quadruple the crushing stress. There is, therefore, an active search for means of obtaining both more efficient heat transfer from the conductor to the cooling medium and of increasing the strength of the conductor without degrading its superconducting or low-normal-resistance properties.

5.2.3 Theta-Pinch Reactor. The supercon-

ducting and associated heat-transfer problems of this confinement system are different in many aspects from either of the systems previously discussed.

The proposed mode of operation of a Theta-Pinch reactor commences with plasma ignition resulting from the first implosion of a magnetic fluid building up to $I = 2.7$ in less than one micro-second. The next phase consists of a "slow" build-up of the field to about $I = 7$ in about another 1 millisecond. The final phase is a slow collapse of the field with an $\#$ decay constant of 60 milliseconds as the compression coil is short-circuited by a "crowbar" switch. Since this sequence of events is repeated every 300 seconds, the Theta-Pinch reactor is very much a pulsed device [1,2].

The initial phase is too rapid for any energy storage system other than fast capacitor banks to be considered. The second phase, in which the majority of the total required energy is transferred, is within the range suited to magnetic energy storage for which the capital cost per

unit is very much less than that for capacitor systems. However, the stored energy is large, 20 MJ in the Los Alamos reference reactor design, and to achieve a net power input, superconductors must be used for these units.

The coil which actually generates the magnetic field in the plasma region must be closely coupled to the plasma and because of the radiation losses alone, it cannot be superconducting. A simplified sequence of operations, for such pulses, is therefore:

- 1) Charge the superconducting storage units during the 300 seconds between pulses.
- 2) Fire the fast implosion capacitor bank.
- 3) Transfer the inductively stored energy into the load. To minimize losses during the energy storage time, the inductors are short-circuited by low-resistance switches situated in the liquid helium. This circuit must be opened to transfer the energy into the load, and to complete the transfer in the required time a peak voltage of 60 kV is impressed across the inductor. Since the "cryogenic" switches are unable to perform this breaking duty, they are backed up by room-temperature vacuum switches which open shortly after the cryogenic switches and, therefore, only carry current for a short time and then interrupt it.
- 4) The coil is shorted by a "crowbar" switch to maintain the current in the coil for 50 ms.
- 5) The "crow-bar" switch is opened and as much of the magnetic field energy as possible is transferred back into the storage coils where any losses are made good from the charging supply during the 300 seconds between pulses.

This proposed use of superconductors poses many severe heat transfer problems. As mentioned earlier, superconductors are only lossless under D.C. conditions. One of the most difficult tasks, therefore, is limiting the overall losses in the complete storage and transfer system to an acceptable value --- remembering that 1 watt at 5 K requires about 300 watts of refrigeration

power. The very fast rate at which the energy is extracted from the storage units, and the limit on losses, requires very special conductors. Very small diameter wires must be used to reduce eddy currents and yet the conductor current is high, typically 75 kA . To meet these requirements, many fine strands must be cabled or woven into a flat strip conductor. Even inside the strands, resistive barriers, usually cupro-nickel, must be incorporated to reduce circulating currents between superconducting filaments which otherwise would produce prohibitive heat loads.

The construction of the energy storage coil is quite different from those previously discussed. The eddy currents losses that would be generated in the copper required for cryostatic stability would vastly exceed the permissible limit. Some low-resistance metal must be included in the conductor strands to prevent turnover in the event that some portion of the superconductor goes "normal". However, since the coil is designed to withstand rapid re-energizing under normal operating conditions, only a small cross-section of copper is necessary for this duty. Since cryostatic stability is disallowed, the system must be designed, built and operated in such a way that any transient heat pulses are insufficient to raise the superconductor to its critical temperature. If a local heat pulse were to raise the conductor temperature above its critical temperature, heat generated by the current flowing in the small copper section would be sufficient to cause the normal region to propagate and the coil to quench. Inter-turn and inter-coil movements under the influence of the magnetic field must be eliminated. The most common approach to solving this problem is to impregnate the coil in epoxy resin. This, however, brings its own problems, such as differential contraction rates, cracking of unfilled resin, and temperature gradients in the coolant. Even a small propagation of a crack in the cured resin while the coil is being stressed as it is energized may easily release sufficient energy in the form of heat to initiate a quench. As a result, coils for this type of duty are still very much in the development stage.

5.3 Protection and Safety. The problems associated with protection and safety of the superconducting coils with their enormous stored energy, about 10^5 MJ for a typical Tokamak, are so enormous and diverse that they can only be briefly touched upon in this paper. A certain amount of experience has already been accumulated in this area but there are enormous differences between the size and potential hazard of existing systems and those envisaged in the future.

The types of fault include:

- a) Sudden failure of the cryogenic vacuum,
- b) Quench of a coil, which may be the whole system, or one of many coupled coils,
- c) Electrical short or open circuits,
- d) Open circuit of a main lead,
- e) Failure of major insulation.

Quenching is the result of a normal zone propagating through the coil. In most coils, its initiation can be detected readily by use of a sensitive voltage sensor connected between a point on the winding, ideally near its center, and a balancing position on a divider connected

across the coil terminals. Under normal conditions and during charging of the coil, the circuit is balanced. If a part of the winding begins to go resistive, the resulting unbalance is detected by the sensor. In most cases, the sensor has variable sensitivity controls to allow it to reject spurious signals but when a genuine quench is indicated, an active energy removal circuit is usually automatically triggered. This involves opening the supply to the coil and allowing the current to decay through an external resistor permanently connected across the coil. The ratio of energy dissipated inside the coil to that in the external circuit is directly proportional to the values of internal and external resistance. While the external value is usually constant, the internal value is continually changing as the normal region propagates (three-dimensionally) and as the resistivity varies throughout the normal region with temperature. Computer programs have been written [5,6] which can now predict, under certain conditions, with reasonable accuracy how the peak coil temperature, internal voltages, and internal and external energy vary with time as the quench proceeds and the total energy is dissipated.

This presents interesting heat transfer problems since the velocity of propagation of the "normal" front along the conductor, from turn to turn and from layer to layer are all different and vary with temperature and, therefore, time. McLock and James [6,13] show how the maximum hot-spot temperature can be calculated if the current density is assumed to be a true exponential (i.e., the coil resistance is negligible compared to the external resistor). They also assume negligible heat transfer to the coolant and that all of the heat generated in the conductor is absorbed by the thermal mass. While this is somewhat pessimistic, the method provides a quick and easy means of determining the amount of stabilizer required to limit the hot-spot temperature to a given value.

While this method of quench detection and energy transference to an external resistor has been found to be quite satisfactory for many systems built to date, it must be studied in much greater depth for the large systems now envisioned. The danger of voltage breakdown during the discharge period becomes an increasing hazard since voltages in general tend to increase with stored energy. Helium, particularly in gaseous form and at higher temperatures, typical of the quench condition, has a very low breakdown strength. Detailed studies will be required during the design phase of these large machines to ensure that breakdown cannot occur along an insulating surface between adjacent turns, or layers, or between a conductor and the retaining case or reinforcing structure. From a breakdown point of view, the conductor should ideally be surrounded by solid insulation which must be punctured before a breakdown can occur. This, however, conflicts with the stability requirement of minimum temperature difference between the conductor and coolant. Satisfactory solutions must be found which meet all requirements with the high degree of reliability expected of a power reactor.

An alternative protection system relies on distributing the total stored energy approximately

uniformly in all of the cold structure rather than extracting it and dumping the majority in an external room-temperature resistance. If this can be achieved, the maximum temperature even in large systems may be limited to something in the region of 70 K. Since there is little thermal expansion between 1 K and 77 K, there are no resulting severe thermal stresses or strains. If higher temperatures are reached, differential thermal expansion could become a serious problem since the structure will most likely be fabricated from stainless steel which has a much longer thermal time constant than that of the conductor.

Methods envisaged of causing the energy to be distributed evenly include:

- 1) Resistance wires in close thermal contact with the conductor throughout its length, through which current can be passed at the onset of a quench and, thus, cause the whole coil to heat up and quench approximately simultaneously.
- 2) A rapid expulsion of all of the liquid helium from the system so that the normal region will propagate much more rapidly due to the poorer cooling properties of the gas. Such a system would probably need to be combined with (1) since in a multi-coil system, propagation might not spread from coil to coil without assistance.

In addition to the problem of disposing of the stored magnetic energy in the event of a fault, questions concerning the behavior of the liquid helium also arise. Initial fears that the liquid would be vaporized so suddenly that a major explosion would occur in a large system now seem unlikely to be realized given reasonable precautions. The process is somewhat self-protecting since a hot surface in contact with the liquid immediately goes into the film boiling regime so that a layer of gas limits the rate at which heat can be transferred to the liquid to vaporize it. In many existing plants, blow-off valves permit the vaporized gas to be evacuated from the tank to a recovery system or to the atmosphere. Many recovery systems consist of low pressure plastic bags from which the gas is later pumped to high pressure for storage in cylinders. In large systems, the sudden influx of so much cold gas would freeze the plastic which would then crack and shatter as it tried to expand. This can be prevented by passing the cold gas through a heat-exchanger to warm the gas before allowing it to enter the bag. A long cylinder filled with granite stone chips has been found to be suitable for this purpose since it is inexpensive, has a high thermal capacity, low time constant and a low pressure drop.

As the helium inventory increases, (e.g., the CMAX-III reactor requires about 550,000 litres), removal in the liquid state is probably more practical, but this now means that the insulation must withstand the discharge voltages in a gaseous helium environment. It also implies that the exhaust lines and storage tanks must be permanently maintained at 4 K to prevent a back pressure from being rapidly built up if the cryogenic fluid were allowed to enter a warm chamber.

SECTION 4. CONCLUDING REMARKS

In this review paper, we have attempted to introduce researchers in the field of heat transfer to some of the interesting and complex heat transfer problems uncovered to date in MFT conceptual design studies. It should be pointed out that these studies have been performed by relatively few people working for only a few years. The first experimental machines which will actually "turn" heat are just now being designed, and we can expect many more heat transfer problems to surface as the detailed designs progress. The expertise of many more thermal-hydraulic system designers, engineers and researchers will be needed in the coming years to solve these problems.

REFERENCES

1. Fuchs, W. J. and Bierman, R. J., "The Importance of 'Fusion Power,'" Scientific American, 1971.
2. Fuchs, W. J., "Concepts and Fusion Research and Development on Liners," Annual Review of Nuclear Science, vol. 21, 1971.
3. Fuchs, W. J., "Fusion Reactor Systems," Nuclear Power, vol. 47 #1, 1975.
4. Fuchs, W. J., "Comparative Study of the Mechanical Properties of Blanket Materials, Power Systems, Systems and Tritium Recovery and Disposal Systems for Fusion Reactors," ORNL/M-3446, Oak Ridge National Laboratory, 1970.
5. Fuchs, W. J., "System Studies of Proposed Fusion Reactors," ORNL/M-3446, Culham Lab., 1974.
6. Fuchs, W. J. and Bohn, Th., "Blanket Cooling Concepts and Heat Recovery Cycles for Controlled Thermonuclear Reactors," Proceedings, Fourth IAEA Conference on Plasma Physics and Controlled Nuclear Fusion Research, Madison, Wisconsin, vol. III, IAEA, IAEA-1971, Vienna, Austria 1971, pp. 160-186.
7. Milley, S., "Fusion Energy Conversion," November 1974 draft, ABC Monograph Series on Nuclear Energy (to be published).
8. Post, R. F., "Mirror Systems: Fuel Cycles, Heat Moderator and Energy Recovery," ORNL/M-3446, Lawrence Livermore Laboratory, 1969.
9. Vair, P. W. and Barr, W. L., "Venetian-Blind Direct Energy Converter for Fusion Reactors," Nuclear Fusion, 1973.
Also: Barr, W. L., et al., "A Preliminary Engineering Design of a Venetian-Blind Direct Energy Converter for Fusion Reactors," IEEE Trans. on Plasma Sci., vol. P-1, 1973.
10. Wood, M. and Weaver, T., "Some Direct Conversion Possibilities for Advanced CTR Systems," ORNL/M-3446, Lawrence Livermore Laboratory, 1973.
11. Grimes, W. R. and Cantor, S., "Molten Salts as Blanket Fluids in Controlled Fusion Reactors," USAEC Report ORNL-IM-1047, Oak Ridge National Laboratory, 1972.
Also: Grimes, W. R. and Cantor, S., "Molten Salts as Blanket Fluids in Controlled Fusion Reactors," in The Chemistry of Fusion Technology, Green, L. M. (ed.), Plenum Press, N.Y. 1973 pp. 161-190.
12. Hoffman, M. A. and Carlson, G. A., "Calculation Techniques for Estimating the Pressure Losses for Conducting Fluid Flows in Magnetic Fields," ORNL-51010, Lawrence Livermore Laboratory, 1971.
13. Hoffman, M. A., "Magnetic Field Effects on the Heat Transfer of Potential Fusion Reactor Coolants," ORNL-73993, Lawrence Livermore Laboratory, 1973.
14. Hunt, J. C. R. and Hancock, R., "The Use of Liquid Lithium as Coolant in a Toroidal Fusion Reactor, Part I. Calculations of Pumping Power," CLM-R112.
15. Hunt, J. C. R. and Booth, J. A., "Part II - Stress Limitations," CLM-R112, Culham Lab., 1971.
16. Hunt, J. C. R. and Sherriff, J. A., High Hartmann Number Magnetohydrodynamics, Annual Reviews of Fluid Mechanics, 3, 1971.
17. Moszynski, J. R., et al., "Cooling of Controlled Thermonuclear Fusion Reactors of Toroidal Configurations," Proceedings, Symposium on Technology of Controlled Fusion, Austin, Texas, 1972.
18. Branser, G. C., et al., "Turbulent Magnetohydrodynamic Flow in Prismatic and Cylindrical Pipes," translated as NASA-TI-F-182, 1967.
19. Coultas, T. A. and Krakowski, R. A., "Aspects of Theta-Finch Powerplant Development," Proc. Fifth Symp. on Eng. Probs. of Fusion Res., Princeton, 1973.
20. Loeffler, A. L., et al., "KED Round Pipe Flow Experiments," USAF-ASL Report 6-0236, 1967.
21. Gardner, R. A. and Lykoudis, P. J., "Magnetofluid-Mechanic Pipe Flow in a Transverse Magnetic Field with and without Heat Transfer," AIAA Paper 69-723, 1969.
22. Jaumotte, A. L. and Hirsch, C., "Ecoulement Magnetohydrodynamique en Conduites," Mechanique Appliquee, 560, 1967.
23. Globe, S., "The Effect of a Longitudinal Magnetic Field on Pipe Flow of Mercury," J. Heat Transfer, Trans. ASME, 445, 1961.
24. Fraim, F. W., "The Effect of a Strong Longitudinal Magnetic Field on the Flow of Mercury in a Circular Tube," Ph.D. Thesis, Massachusetts Institute of Technology, 1966.

1.11 Gardner, R. A., "Laminar Pipe Flow in a Transverse Magnetic Field with Heat Transfer," *Int. J. Heat Mass Transfer*, 11: 1076, 1968

1.12 Kovner, D. C., et al., "Experimental Study of the Effect of a Longitudinal Magnetic Field on Convective Heat Transfer in a Turbulent Pipe Flow of Conducting Liquids," *Magnetohydrodynamics*, 10, pp. 30-37, 1966

1.13 Carlson, G. A., "Magnetohydrodynamic Pressure Drop of Lithium Flow in a Inducting Wall Pipe in a Transverse Magnetic Field—Theory and Experiment," UCRL-7537, Lawrence Livermore Laboratory, 1971

Also: Proc. of the First Topical Meeting on the Tech. of Controlled Nuclear Fusion, UCNP-100-1-1, USAEC, San Diego, 1970

1.14 The University of Wisconsin Fus. & Plasma Physics Group, "A Wisconsin Toroidal Inductron Reactor Design," UCNP-100-66, 1970

1.15 Ho, L. H. and Stewart, W. E., "Experimental and Mechanical Design of a Helium-cooled Lithium Reactor Blanket," *Proc. of FUSC Symp. on Inst. Probs. of Fusion Res.*, Princeton, 1970

1.16 Werner, R. W., et al., "Progress Report #2 on the Design Considerations for a Low Power Experimental Mirror Fusion Reactor," UCRL-75113, Lawrence Livermore Laboratory, 1971

1.17 Mitchell, J. T. D. and Harrold, R., "A Tritium-Cooled Corotating Fusion Reactor" UCRL-75114, 1972

Also: Penberthwait, J. S., et al., "Design of Stainless Steel Blanket Cells for a Fusion Reactor," UCRL-5127, Culham Laboratory, 1971

1.18 Miller, R. J. (Ed.), "A Fusion Power Plant," WAT-1051, Plasma Physics Laboratory, Princeton University, 1972

Also: Davidson, P. H., "Optimization of the Design for Cooling the Breeding Blanket of the Princeton Reference Reactor Model of a Fusion Power Reactor," *Proceedings, Symposium on Technology of Controlled Fusion, Austin, Texas*, 1973

1.19 Werner, R. W., "The Module Approach to Blanket Design—Vacuum Wall Free Blanket Using Heat Pipes," UCRL-75758, Lawrence Livermore Laboratory, 1969

1.20 Carlson, G. A. and Hoffman, M. A., "Effect of Magnetic Fields on Heat Pipes," UCRL-72050 Rev. 1, Lawrence Livermore Laboratory, 1970

2.30 Frass, A. P., "Analysis of a Recirculating Lithium Blanket Designed to Give a Low Magnetohydrodynamic Pumping Power Requirement," USAEC Report ORNL-DM-3756, Oak Ridge National Laboratory, 1972

2.31 Frass, A. P., "Conceptual Design of the Blanket and Shield Region and Related Systems for a Full-Scale Toroidal Fusion Reactor," USAEC Report ORNL-TM-3096, Oak Ridge National Laboratory, 1973

2.32 Carlson, G. A., "Electromagnetic Pumping to Eliminate NHD Pressure Drops in Fusion Reactor Blankets," UCID-16029, Lawrence Livermore Laboratory, 1972

2.33 Young, F. J., et al., "Magnetohydrodynamic Test of a One-Sixth Scale Model of a CTR Recirculating Lithium Blanket," USAEC Report ORNL-TM-1618, 1973

2.34 Frass, A. P., et al., "Effects of a Strong Magnetic Field on Boiling of Potassium," DPRL-TM-1215, Oak Ridge National Laboratory, 1971

2.35 Hopkins, G. R. and Nease-d'Hospital, G., "Direct Helium Cooling Cycles for a Fusion Reactor," GA-3649, Gulf General Atomics, San Diego, CA, 1969. Also see *Proceedings, Nuclear Fusion Reactors Conference, JAEA, Culham, England*, 1969 pp. 322-330

2.36 Nease-d'Hospital, G. and Hopkins, G. R., "Gas Cooling for Fusion Reactor Blankets," 5th International Energy Conversion Eng. Conf., Las Vegas, Nevada, in Energy '70: Fusion Technology, Myers, B. (Ed.), Lawrence Livermore Laboratory, 1970, pp. 1-6, to 1-71.

2.37 Hoffman, M. A., et al., "Parametric Study of Helium Cooling and Associated Engineering Problems of Future Fusion Reactors," Proc. of Fifth Symp. on Eng. Probs. of Fusion Res., Princeton, 1973

2.38 Frass, A. P., "Problems in Coupling a Gas Turbine to a Thermonuclear Reactor," AERE Paper HE-296, 1972

2.39 Mitchell, J. T. D. and Booth, J. A., "Wall Loading Limitations in a Helium Cooled Fusion Reactor Blanket," UCRL-51270, USAEC Research Group, Culham Laboratory, Paper No. 13 of Workshop of Fusion Reactor Design Problems, 1971

2.40 Moir, R. W., et al., "Progress in the Conceptual Design of a Mirror Hybrid Fusion-Fission Reactor," UCRL-51797, Lawrence Livermore Laboratory, 1975

2.41 Bertolini, E., et al., "Design of a Minimum Size Toroidal D-T Experimental Reactor," JAEA-CX-33-G1-1, Laboratori Nazionali del CNE, Frascati, Italy

Also: Biggio, M. et al., "Blanket Problems Related to Demonstration Fusion Power Reactors," Proc. of Fifth Symp. of Eng. Probs. of Fusion Res., Princeton, 1973

2.42 Powell, J. R., et al., "Studies of Fusion Reactor Blankets with Minimum Radioactive Inventory and with Tritium Breeding in Solid Lithium Compounds: A Preliminary Report," PHL-16236, Brookhaven National Laboratory, 1973

4.32 Peterson, M. A., et al, "A Modularized Mirror Fusion Reactor Concept With Emphasis on Fabrication, Assembly, and Disassembly," UCRL-74076, rev 1, 1971, Lawrence Livermore Laboratory, 1971

4.33 Sato, T. K., et al, "A Gas-Carried Li D Cooling-Breeding Fusion Reactor Blanket Concept," Fusion Technology Program, U. Wisconsin, 1977

4.34 Baker, R. E., et al, "UNMAK-II, A Conceptual Tokamak Power Reactor Design," University of Wisconsin, Report UNFDM-111, 1975

4.35 John, R. W., et al, "Preliminary Design Aspects of the UNMAK-II Conceptual Tokamak Power Reactor," Transactions of the AIC, vol 12 pp. 99, 1975

4.36 Baxton, J. H., et al, "Conceptual Design of a Mirror Reactor for a Fusion Engineering Research Facility (FERF)," Lawrence Livermore Laboratory, UCRL-74017, 1974

4.37 Conn, R. W., et al, "New Concepts for Controlled Fusion Reactor Blanket Design," University of Wisconsin, UNFDM-115, 1974

4.38 Hoffman, M. A., et al, "Fusion Reactor First-Wall Cooling for Very High Energy Fluxes," Lawrence Livermore Laboratory, UCRL-75820, 1974

4.39 Werner, R. W., "Thermonuclear Reactors, Mirror Machines and Direct Conversion," UCRL-72969, 1971

4.40 "Status and Objectives of Tokamak Systems for Fusion Research," KASH-1295, USABC, 1974

4.41 Mills, R. G., "A Fusion Power Plant," Princeton Plasma Physics Lab., MATT-1050, 1971

4.42 "Wisconsin Tokamak Reactor Design UNMAK I," University of Wisconsin, UNFDM-68, 1974

4.43 Werner, R. W., et al, "Progress Report #2 on the Design: Considerations for a Low Power Experimental Mirror Fusion Reactor," UCRL-74051-2, Lawrence Livermore Laboratory, 1974

4.44 Fuchs, A., "Tinsema Physics," 14, pp. 211, 1970

4.45 Koir, R. W. and Barr, W., "Venetian Blind Direct Energy Converter for Fusion Reactors," Nuclear Fusion 13, pp. 35, 1973

4.46 Lee, J. D., et al, "Mirror Reactor Blankets," Lawrence Livermore Laboratory, UCID-17083, 1976

4.47 "Operating Modes and Trade Offs for Mirror Fusion Reactors," Condit, 1975, Lawrence Livermore Laboratory, UCIR-962

4.48 Corder, J. G. and Watson, C. J. H., "Toroidally Linked Mirror Reactor Design," Culham Laboratory, IAEA, Workshop on Fusion 1973

4.49 "UNMAK-II, A Conceptual Tokamak Reactor Design," University of Wisconsin, UNFDM-112, 1975

4.50 Kodatany, B. E., et al, "Some Unsolved Problems Most Essential to Physics and Technology of Fusion Reactors," IAEA Workshop on Fusion, 1973, Culham Laboratory, UK

4.51 Haas, J., et al, "Impurity Problems Operating in Quasi Steady State Toroidal Flame Experiments and Fusion Reactors," paper #3C, Max Planck Institut for Plasmaphysik

4.52 Baxton, J. H., et al, "A Peloidal Divertor for the UNMAK-II Reactor," University of Wisconsin, 1974

4.53 Kondratenko, N., "Surface Effects in Thermonuclear Devices and Reactors," Argonne National Laboratory, 7th Symposium on Fusion Technology, Grenoble France, 1972

4.54 Barr, W. L., et al, "A Preliminary Engineering Design of a 'Venetian-Blind' Direct Energy Converter for Fusion Reactors," IEEE Transactions on Plasma Science, vol. PI-2, 1974

4.55 Post, S. F., "Mirror Systems: Fuel Cycles, Loss Reduction and Energy Recovery," Proceedings of Nuclear Fusion Reactors Conference, pp. 35, Culham Laboratory, UK 1969

4.56 Barr, W. L., "Some Considerations in the Design of a Venetian Blind Direct Converter," UCID-16985, 1975

4.57 Gough, W. J., "The Technology of Divertors," USABC, Division of Research, 1976

4.58 "IAEA Workshop on Fusion Reactor Design Problems," Culham Laboratory, UK, 1971

4.59 "Proceedings of the Sixth Symposium on Engineering Problems of Fusion Research," San Diego, CA, 1975, Sponsored by General Atomic, IEEE, ERDA, and AIAA

4.60 Werner, R. W., et al, "Progress Report #2 on The Design Considerations for a Low Power Experimental Mirror Fusion Reactor," UCRL-74051-2, Lawrence Livermore Laboratory, 1974

4.61 Coenagin, F., et al, "Physical Review," Letters, vol. 35 pp. 1501, Journal 22, 1975

4.62 "MX Draft Proposal," UCID-17025

5.1 Cobb, R., et al, "University of Wisconsin UNMAK-III Design Report," UNFDM-150, 1975

5.2 McCracken, J. M. and Blov, S., "The Shielding of Superconducting Magnets in a Fusion Reactor," Culham Lab., Report CLM-R120, 1972

5.1 Lubell, M. S., "State-of-the-art of Superconducting Magnets," ORNL Report TM-1961, 1972

5.2 Arp, V., et al, "Helium Heat Transfer," National Bureau of Standards, Boulder, Report 17753, 1972

5.3 Morpurgo, M., "The Design of the Superconducting Magnet for the Omega Project," Particle Accelerators, 1970, vol. 1, Gordon and Breach, Science Publishers, Ltd.

5.4 Hoenig, M. J. and Montgomery, F. J., "Dense Superconducting-Helium Cooled Superconductors for Large High Field Stabilized Magnets," Proc. Transactions of Magnetics, v.1, "MAG-11, 1975", 1975

5.5 Carlson, G. A. and Moir, R. W., "Mirror Fusion Reactor Study," Proc. ANS San Francisco, 1974

5.6 Rogers, J. D., et al, "Parameter Study of Theta-Vinch Plasma Physics Reactor Experiment," Proc. Fifth Symposium on Engineering Problems of Fusion Research, Princeton, 1973

5.7 Wilson, M. K., "QUENCH" computer program, private communication

5.8 Maslock, B. J. and James, B. A., "Protection and Utilization of Large Superconducting Cables," Proc. IEEE "71 115, no. 4, 1963

214 *Journal of Health Politics*

JOURNAL OF POLYMER SCIENCE: PART A-1

THEORY OF THE BOUND STATE

THE JOURNAL OF CLIMATE

Parameter	Initial value	Final value
Initial temperature	300	470
Initial pressure	100	100
Initial particle density	100	400
Initial particle radius	100	500
Initial particle velocity	100	100
Initial temperature profile	100	100
Initial pressure profile	100	100
Initial particle density profile	100	100
Initial particle radius profile	100	100
Initial particle velocity profile	100	100
Initial temperature profile	1000	1000
Initial pressure profile	1000	1000
Initial particle density profile	1000	1000
Initial particle radius profile	1000	1000
Initial particle velocity profile	1000	1000

TABLE 3.4
COMPARATIVE STUDY OF SEVERAL PROMISING COOLANT
IN A SIMPLIFIED TOROIDAL REACTOR EMPLOYING A
DUCTED COOLANT DESIGN (From Ref. 2.13*)

* mean design parameters:
 Total wall loading, $A_t = 1.0 \text{ m}^2/\text{m}^2$
 Fraction of power to first wall coolant tubes = 0.30
 tube inner diameter, $D_i = 0.025 \text{ m}$
 tube length along first wall = 2.5 m
 Total tube length perpendicular to B₀, $L_t = 12 \text{ m}$
 Mean magnetic field strength = 10 tesla
 tube wall electrical conductivity, $\sigma_w = 1.0 \times 10^6 \text{ mho/m}$
 tube wall thickness-to-radius ratio, $\delta_w/R = 0.35$
 coolant bulk temp. rise along first wall, $\Delta T_{g(V_0)} = 7^\circ \text{C}$

Liquid Li	Liquid (Saturated) H ₂ O	Liquid (Non-boiling) K	Liquid PbTe	Builing Liq. in. ($x = 0$)	Builing Vapor out ($x = 1$)	Builing Liq. in. ($x = 0$)	Builing Vapor out ($x = 1$)	ΔP (psi)
1.09 (1.09)	0.61 (0.60)	0.61 (0.60)	0.38 (0.37)	0.001 (1,570)	94 (variable)	0.261 (10,000)	0.6 (variable)	30
1.10 (1.10)	0.60 (0.60)	0.60 (0.60)	0.38 (0.37)	0.001 (1,570)	94 (variable)	0.261 (10,000)	0.6 (variable)	30,000
Water (saturation 3.4, E_0)	0.60 (0.60)	0.60 (0.60)	0.38 (0.37)	0.001 (1,570)	94 (variable)	0.261 (10,000)	0.6 (variable)	0
Wall conductance ratio, G	0.05 (0.05)	0.05 (0.05)	0.05 (0.05)	0.025 (0.025)	~ 0 ~ 0	~ 0 ~ 0	~ 0 ~ 0	~ 0
Friction drop, ΔP_{fr}	0.30 (0.30)	0.30 (0.30)	0.30 (0.30)	0.2 0.2	1.0 0.61	260 0.03	0.4 0.000	0.4
Boiling power ratio, $P_{L,liq}/P_{L,vap}$	0.05 (0.05)	0.05 (0.05)	0.05 (0.05)	8 8	8 (variable)	8 (variable)	95 95	

* All values taken directly from Ref. 2.13 - except those estimates given in parentheses.

** This is the minimum velocity required for heat removal at first wall.

Table 4.1. A Comparison of Air Liquifiers

Air Liquification System	Work Required to Liquify 1 lb	
	kwh	J/kg
Ideal reversible process	0.095 (Calculated)	7.52×10^5
Hampson or simple Linde process	1.3 (Observed)	1.03×10^7
Hampson precooled to -45°C	0.7 (Observed)	5.54×10^6
High-pressure Linde	0.8 (Observed)	6.34×10^6
High-pressure Linde precooled to -45°C	0.4 (Observed)	3.57×10^6
Claude	0.4 (Observed)	
Heylandt	0.4 (Observed)	3.33×10^6
Ios Alamos cascade (Ball)	0.61 (Observed)	3.25×10^6
Cascade system of Keesom	0.30 (Calculated for N_2)	2.14×10^6

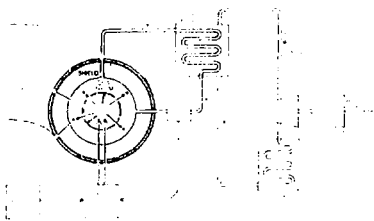


Figure 1.1 Principal components of a Magnetically-confined Controlled Thermonuclear Reactor (MCTR) Powerplant (Ref. 1.1).

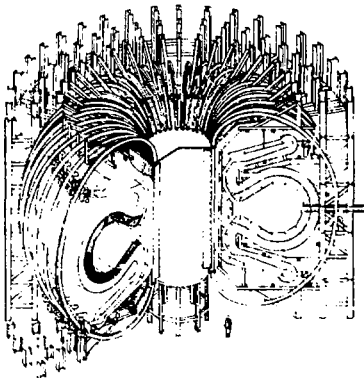


Figure 1.2 Typical Tokamak conceptual design. (Princeton Plasma Physics Lab.).

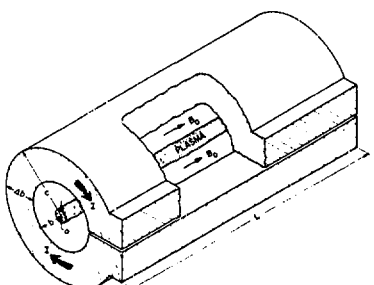


Figure 1.3 Small section of a typical Theta-Pinch plasma and coil. (Los Alamos Scientific Lab.).

Case	Blanket	Nature of cooling material	Intermediate use		Power, CEC PS
			Direct	Indirect	
1	Li	Li (Fibrel)	none	H ₂ O	...
2	Li	H ₂ O	none	H ₂ O	...
3	Li	He	none	H ₂ O	...
4	Li	He	Acne	He	...
5	Li	Li (Fibrel)	none	K	H ₂ O
6	Li	K	none	K	H ₂ O
7	Li	Elbe	none	K	H ₂ O

Figure 2.1 Selected combinations of possible fusion reactor fertile materials; blanket coolants and power cycles (modified version, Ref. 2.3).

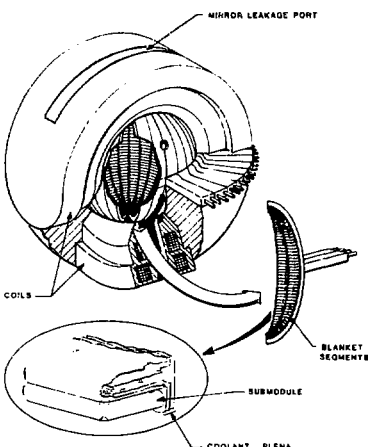


Figure 1.4 Typical Mirror Machine conceptual design. (Lawrence Livermore Lab.).

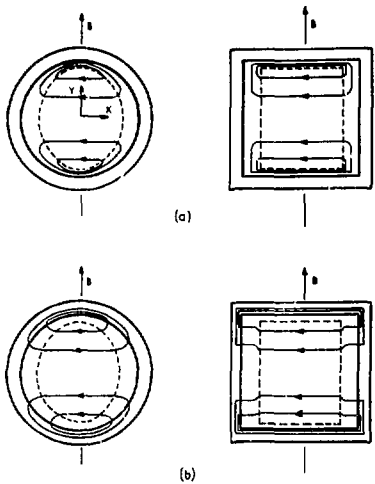


Figure 2.2 Electric Hartmann-type current paths in ducts due to a strong transverse magnetic field. The velocity U_0 is in the z direction, out of the page. (a) Ducts with non-conducting walls. (b) Ducts with highly conducting walls. (Ref. 2.11a).

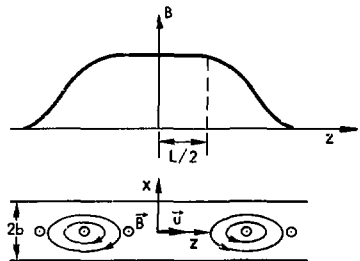


Figure 2.4 End-loop type eddy currents in a region of changing transverse magnetic field (Ref. 2.9).

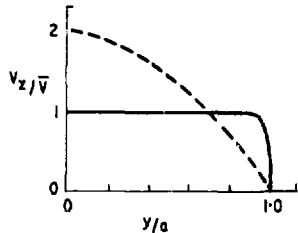


Figure 2.3 Typical velocity profiles in ducts with zero (---) and strong (—) transverse magnetic fields. (Ref. 2.11a).

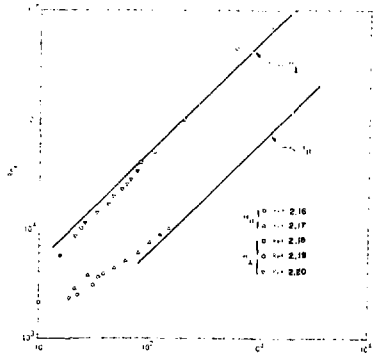


Figure 2.5 Transition Reynolds Numbers for flows of conducting fluids in circular pipes in parallel and transverse magnetic fields (Ref. 2.9).

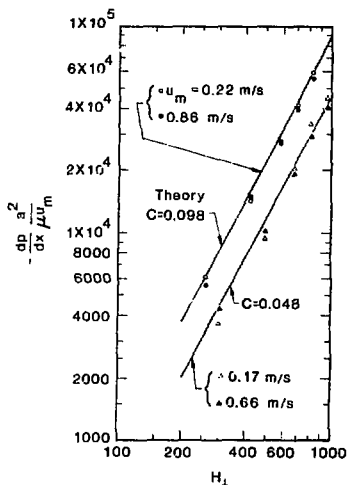


Figure 2.6 Magnetohydrodynamic pressure gradient - theory and experiment. (Ref. 2.23).

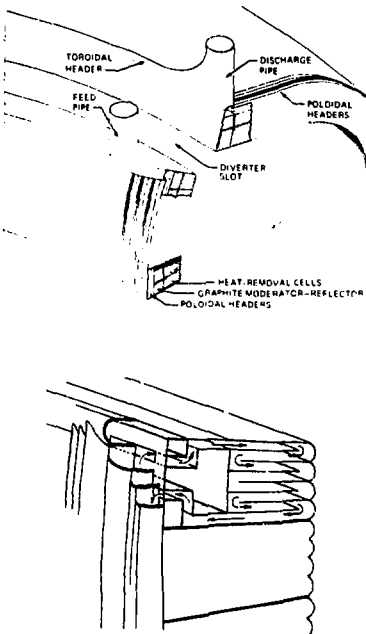


Figure 2.7 Details of the lithium-cooled UMK-I blanket (Ref. 2.24).

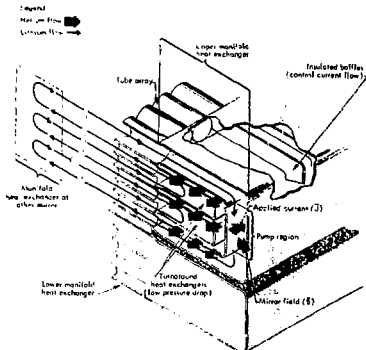


Figure 2.8b Detail of the lithium flow turnaround region of a mirror reactor conceptual design study (Ref. 2.25).

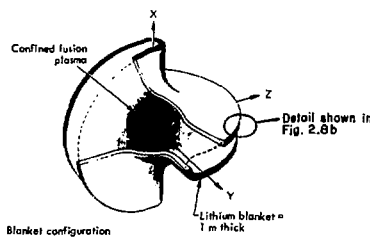


Figure 2.8a General blanket configuration for a mirror reactor conceptual design study (Ref. 2.25).

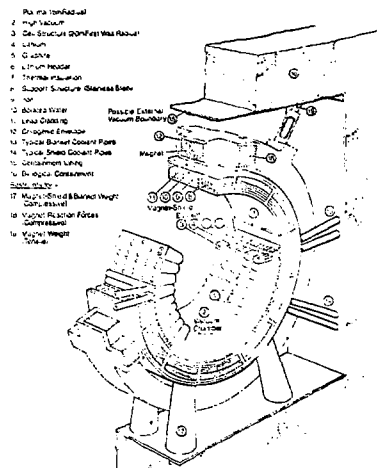


Figure 2.9a Fusion Reactor Blanket and Magnet - General Arrangement of the Culham Tokamak Conceptual design (Ref. 2.26).

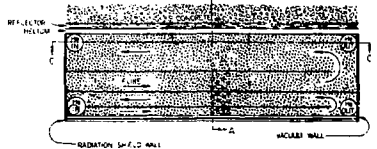


Figure 2.10 Coolant tubes and flow paths in the blanket for the Princeton Fusion Reactor (Ref. 2.27).

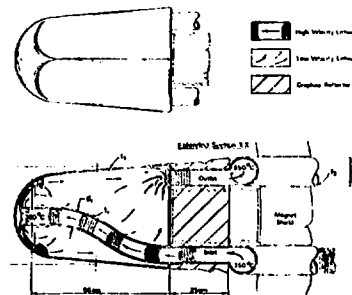


Figure 2.9b Hexagonal Cell Structure for Lithium Fusion Reactor Blanket of the Culham Tokamak fusion reactor conceptual design (Ref. 2.26).

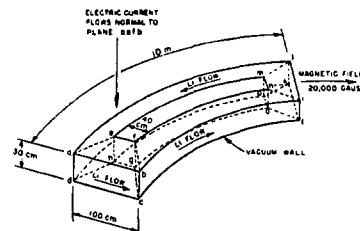


Figure 2.11 Schematic diagram showing the lithium flow through the racetrack-shaped loop in the blanket segments of the ORNL Tokamak reactor design (Ref. 2.31).

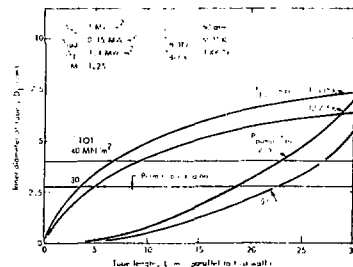


Figure 2.12 Approximate limitations on cooling tube dimensions for a lithium blanket cooled by helium gas flowing in niobium tubes. (Ref. 2.36).

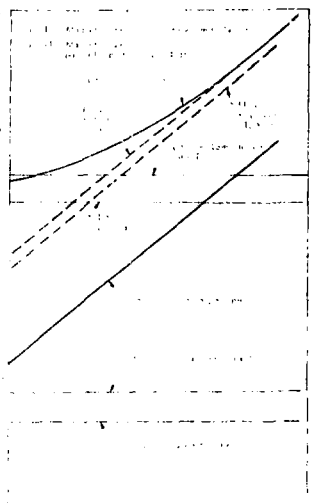


Figure 2.17 Heat transfer parameter comparison for several possible fusion reactor coolants (Ref. 2.10).

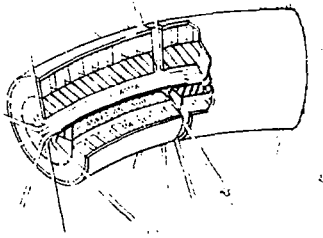


Figure 2.18 Ducted-coolant reference blanket design used for comparison of various coolants (Ref. 2.13).

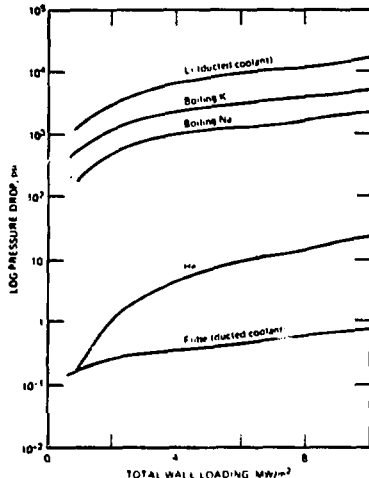


Figure 2.19 Comparison of the pressure drops of various coolants in the ducted-coolant blanket design of Fig. 2.18 (Ref. 2.13).

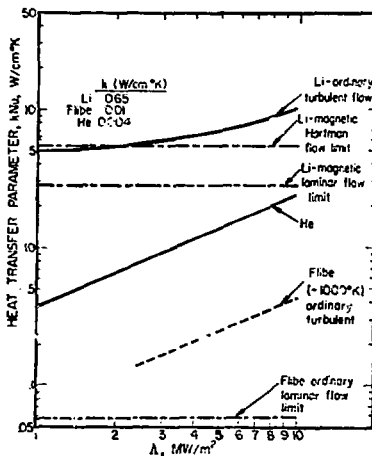


Figure 2.20 The heat transfer parameter, $k \times \text{Nu}$, for the ducted-coolant blanket design of Fig. 2.18 (Ref. 2.4).

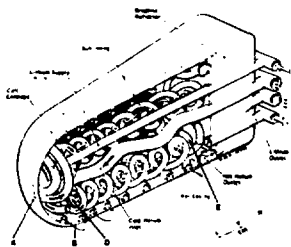


Figure 2.13 Conceptual design of helium-cooled cell for the Culham fusion reactor. (Ref. 2.38).

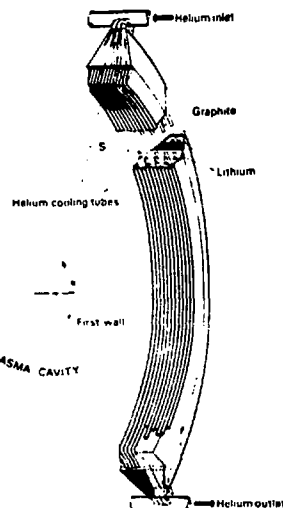


Figure 2.15 Perspective view of a module for a toroidal blanket with helium cooling (Ref. 2.40).

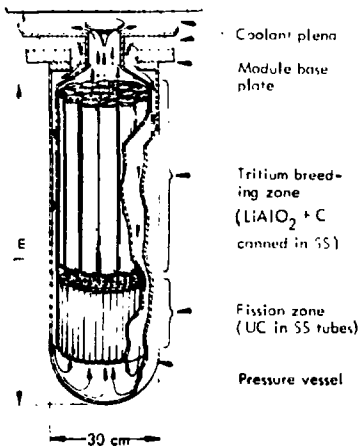


Figure 2.14 Details of the LLL fusion-fission hybrid mirror reactor conceptual design (Ref. 2.39).

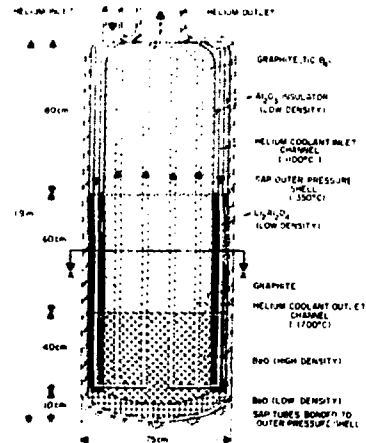


Figure 2.16 Brookhaven design of a helium-cooled blanket module having an aluminum alloy structure and a solid aluminum-lithium alloy as the fertile material (Ref. 2.41).

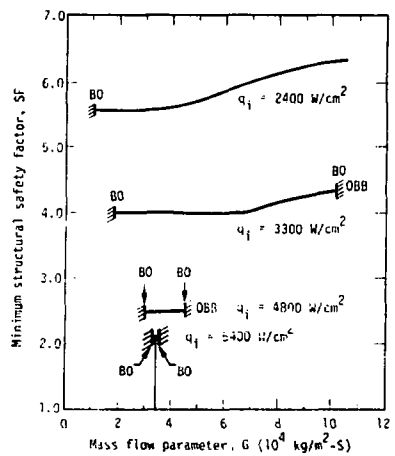


Figure 3.1 Heat flux limitations on a reference first wall shield design (Ref. 3.5).

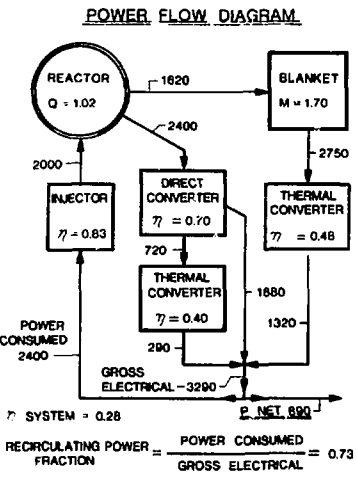


Figure 4.1 Power flow diagram for a mirror reactor with direct conversion.

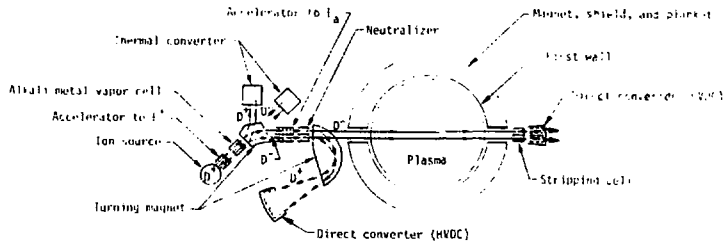


Figure 4.2 Schematic of a mirror machine illustrating the principal components of a negative ion injector.

	Phase 1		Phase 2	Phase 3			
1.0 Sec. Tran. Form er Off Reset	10 Sec. Current Rise Time	10 Sec. * Heating to Operating Conditions	90 Minute Burn Period	1.32 Secs. Plasma Current Decrease	1.0 Secs. Chamber Purge	1.0 Secs. Tran. Form er Off Reset	10 Sec. Current Rise Time

Time →

- * 1.0 SW 750 kWe nominal beam at 250 keV deuterium injector

Figure 4.3 ONE OPERATING CYCLE FOR UMFRE II

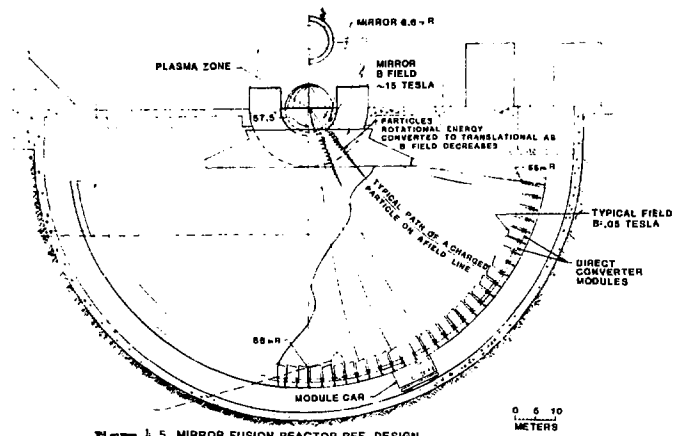


Figure 4.5 MIRROR FUSION REACTOR REF. DESIGN

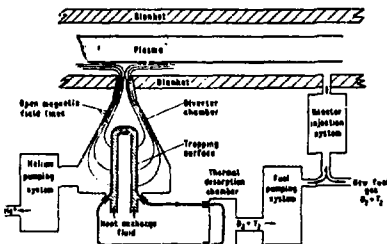


Figure 4.4 Schematic diagram of a fusion reactor divertor

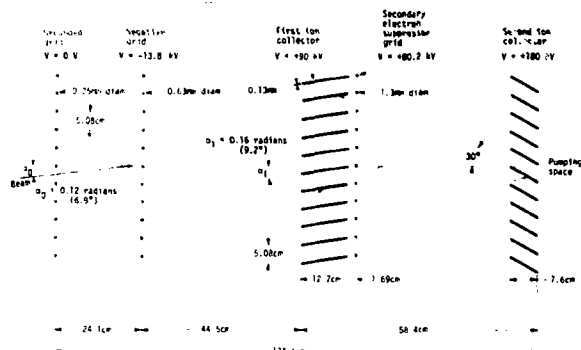


Figure 4.6 Collector and grid array for the Venetian blind converter. The pair of wire grids at the left reflects the electrons and allow ions to pass on through. The Venetian blind appears transparent to the incoming ions but opaque to the ions reflected by the second collector.

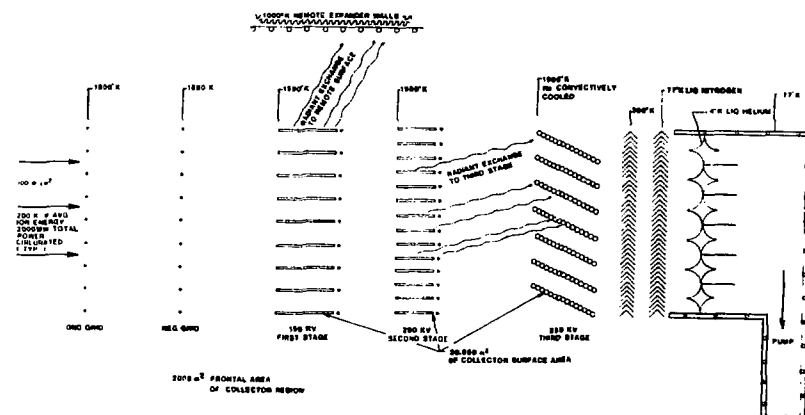


Figure 4.7 HEAT TRANSFER MODEL OF A DIRECT CONVERTER

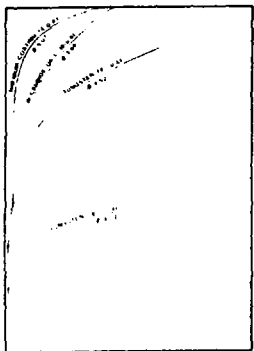


Figure 4.8 Efficiency of direct converter vs. max power density as influenced by thermionic emission of the negative grid wire.

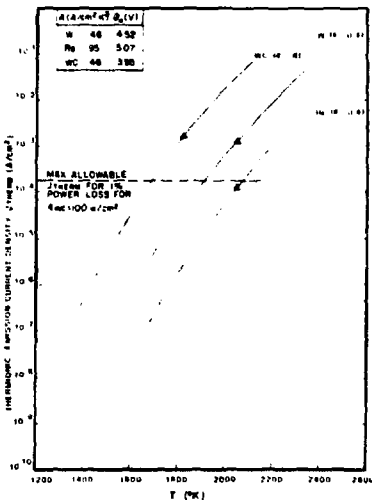


Figure 4.9 Temperature limits due to thermionic emission losses for various grid wire materials

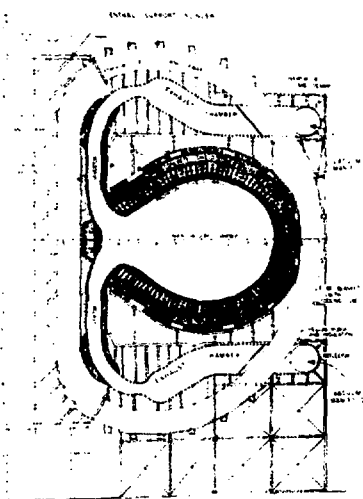


Figure 4.11 Cross section of the Nuclear Island (From PPPL reference design)

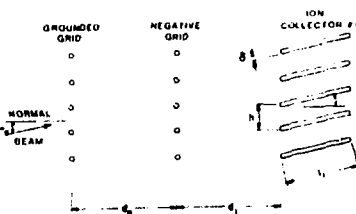


Figure 4.10 The basic dimensions in a Venetian Blind direct converter.

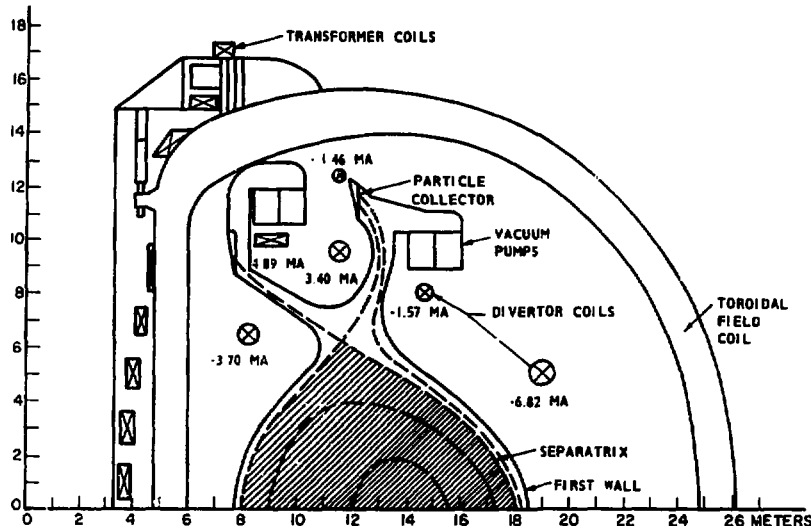


Figure 4.12 UWMAK - II POLOIDAL DIVERTOR

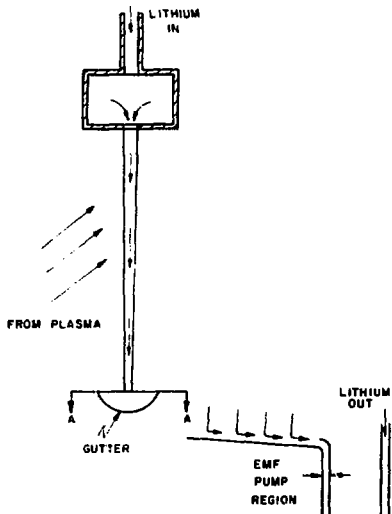


Figure 4.13 Flowing lithium sheet for recovery of diverted D and T. (From UWMAK II)

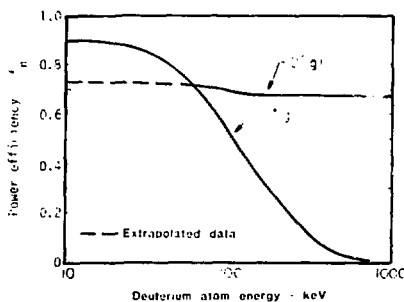


Figure 4.15 Neutralization efficiency as a function of energy of D^+ and D^- .

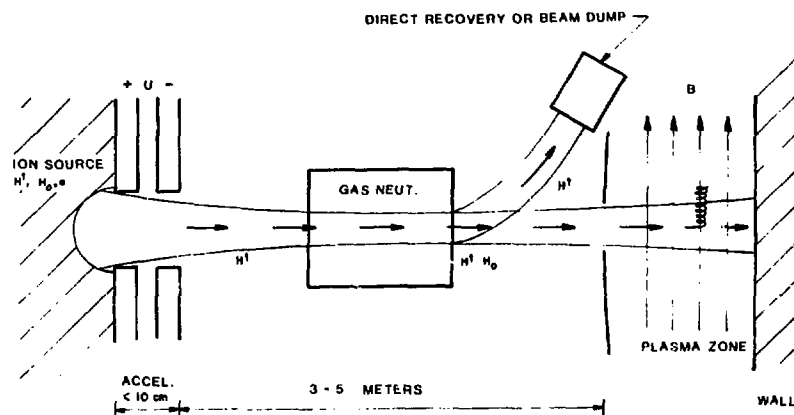


Figure 4.14 PRINCIPLE OF OPERATION OF A POSITIVE ION ACCELERATOR-Injector

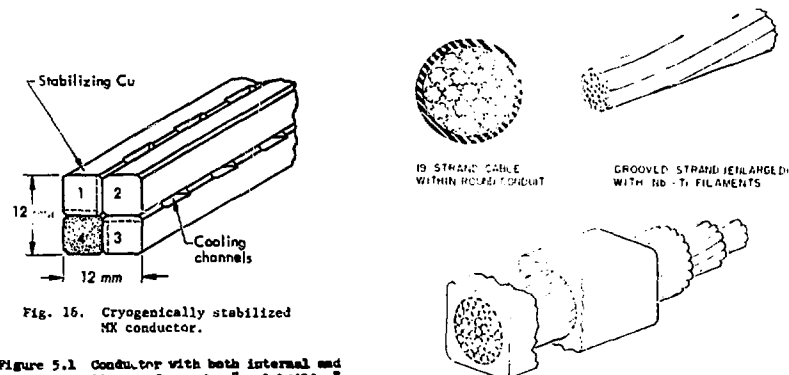


Fig. 5.1. Cryogenically stabilized Nb conductor.

Figure 5.1 Conductor with both internal and external cooling surfaces for "pool boiling" system.

ROUND BUNDLE WITH 37 STRANDS ENCLOSED IN RECTANGULAR CONDUIT - SHOWING TRANSPOSITION OF STRANDS

Figure 5.2 Conductor for internal "forced convection" cooling only.